

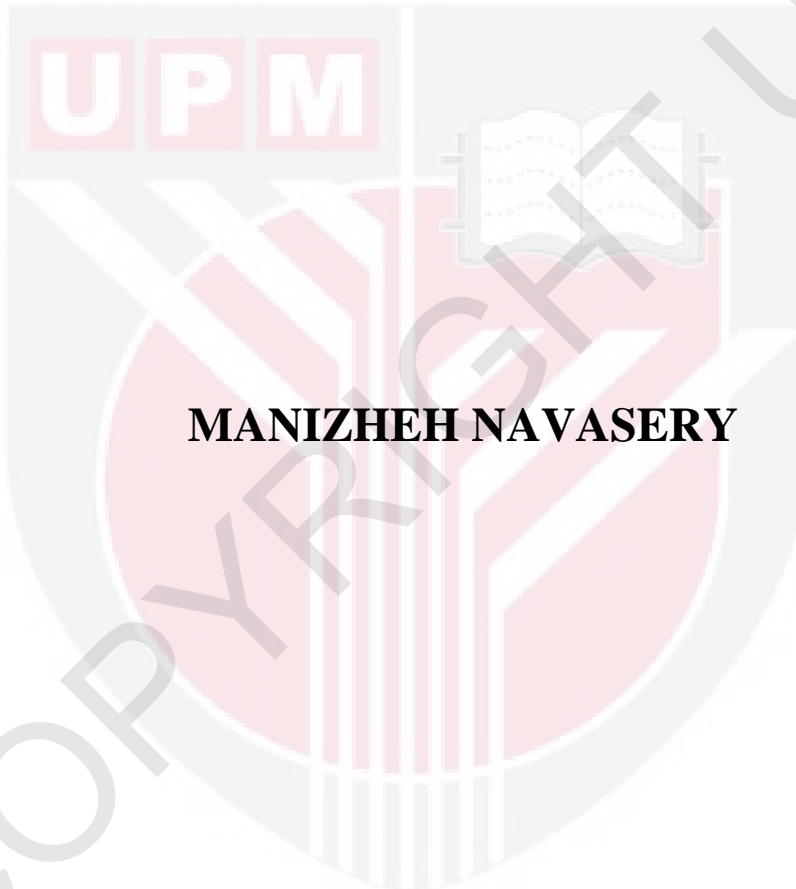


**FABRICATION AND CHARACTERIZATION OF COLOSSAL  
MAGNETORESISTANCE MANGANITES IN BULK, SINGLE LAYER AND  
TRILAYER THIN FILMS PREPARED BY PULSED LASER DEPOSITION  
TECHNIQUE**

**MANIZHEH NAVASERY**

**FS 2012 102**

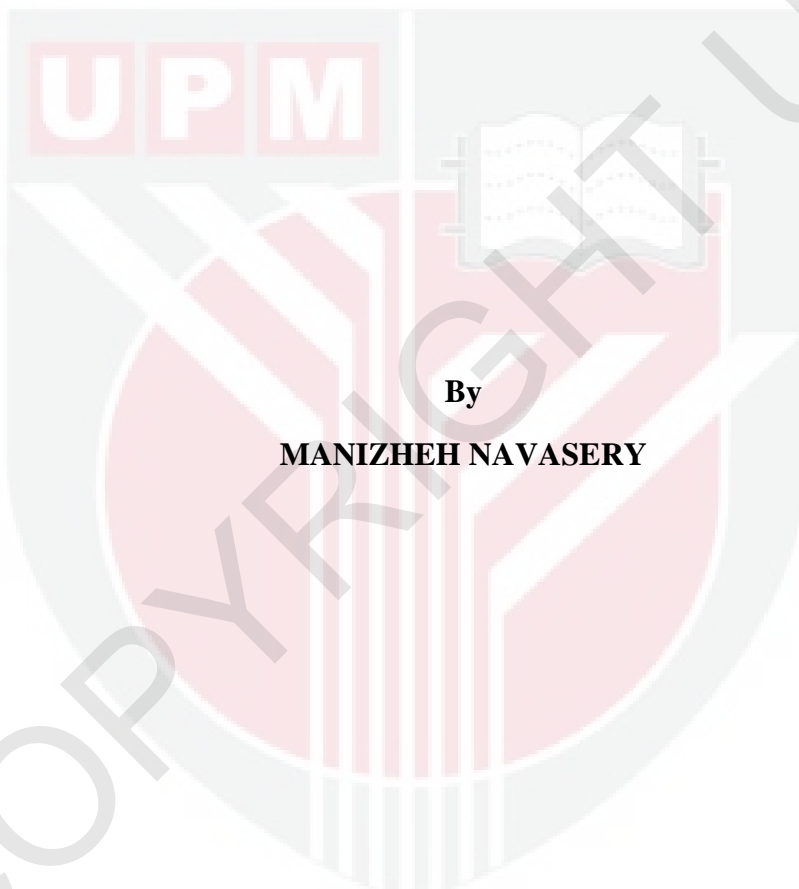
**FABRICATION AND CHARACTERIZATION OF  
COLOSSAL MAGNETORESISTANCE  
MANGANITES IN BULK, SINGLE LAYER AND  
TRILAYER THIN FILMS PREPARED BY PULSED  
LASER DEPOSITION TECHNIQUE**



**DOCTOR OF PHILOSOPHY  
UNIVERSITI PUTRA MALAYSIA**

**2012**

**FABRICATION AND CHARACTERIZATION OF COLOSSAL  
MAGNETORESISTANCE MANGANITES IN BULK, SINGLE LAYER AND  
TRILAYER THIN FILMS PREPARED BY PULSED LASER DEPOSITION  
TECHNIQUE**



**Thesis submitted to the school of Graduate Studies, Universiti Putra Malaysia,**

**In Fulfillment of the Requirement for the Degree of Doctor of Philosophy**

**NOVEMBER 2012**

## Dedication

**To My Mother**

**From Earth to Heaven...**

The words cannot describe how much I missed her. I lost her at a time when I was studying abroad.



Abstract of thesis presented to the Senate of Universiti Putra Malaysia, in Fulfillment of  
the Requirement for the Degree of Doctor of Philosophy

**FABRICATION AND CHARACTERIZATION OF COLOSSAL  
MAGNETORESISTANCE MANGANITES IN BULK, SINGLE LAYER AND  
TRILAYER THIN FILMS PREPARED BY PULSED LASER DEPOSITION  
TECHNIQUE**

By

**MANIZHEH NAVASERY**

November 2012

**Chairman: Abdul Halim Shaari, PhD**

**Faculty: Science**

Electronic and magnetic properties of mixed-valent manganites,  $Re_{1-x}M_xMnO_3$  ( $Re$  = rare earth,  $M$  = alkaline earth), have received a lot of attention in the last decade because of the variety of interesting phenomena exhibited by these materials. This project was aimed at studying the structure and magnetotransport properties of manganites in the form of bulk, single and trilayer thin films prepared by Pulsed Laser deposition (PLD) technique by using Nd-YAG laser on different substrates. A comparison study between the bulk and thin film and the effect of substrate type on the structure, morphology and magneto-transport properties of the thin films was studied. In addition the enhancement of magnetoresistance (MR) and phase transition temperature ( $T_P$ ) on trilayer films are investigated. In the first part, the polycrystalline targets of  $La_{2/3}Ca_{1/3} MnO_3$  (LCMO),  $La_{5/8}Sr_{3/8}MnO_3$  (LSMO),  $La_{0.7}Na_{0.3} MnO_3$  (LNMO) and  $Pr_{0.7}Ca_{0.3} MnO_3$  (PCMO) were prepared by solid state

reaction. All samples were characterized by X-ray diffraction (XRD, Philips). The XRD data were analyzed by Rietveld refinement technique. It was found from XRD results that the bulks (same as thin films) were single phase with the orthorhombic Pnma structure for LCMO and PCMO and rhombohedral  $\bar{R}\bar{3}C$  structure for LSMO and LNMO, where no detectable impurities were observed. A four point probe system which is inserted in the liquid nitrogen cryostat was used to measure the phase transition temperature  $T_P$ , and magnetoresistance of samples by using Hall effect system. LCMO shows metal-insulator transition at 274 K while PCMO is an insulator. In the case of LSMO and LNMO Transition temperature  $T_P$  was above room temperature. The Curie temperature was measured using the CryoBIND T AC Susceptometer.  $T_C$  is found from the peak in the  $d\chi'/dT$  (where  $\chi'$  is the real part of the susceptibility) via temperature curve.  $T_C$  is 94.18 K for PCMO, 330.4 2 K for LSMO, 319.79 K for LNMO and 285.76 K for LCMO manganite bulks. The PCMO sample is insulating at zero magnetic field, and has a charge ordering transition around 200 K followed by antiferromagnetic and ferromagnetic transitions respectively at 142.21 K and 94.18 K that were obtained from the real and imaginary part of AC susceptibility measurement respectively. Finally, by using the vibrating sample magnetometer (VSM, Lake shore 7400) at the maximum magnetic field (10 KG), the magnetization value was 46.24 emu/g for LSMO, 21.45 emu/g for LNMO, 5.49 emu/g for LCMO and  $1.66 \times 10^{-3}$  emu/g for PCMO bulk manganites . In the second part of this work, the manganite targets of  $\text{La}_{2/3}\text{Ca}_{1/8}\text{MnO}_3$  (LCMO),  $\text{La}_{5/8}\text{Ca}_{3/8}\text{MnO}_3$ ,  $\text{La}_{0.3}\text{Na}_{0.7}\text{MnO}_3$  (LNMO) and  $\text{La}_{5/8}\text{Sr}_{3/8}\text{MnO}_3$  (LSMO) were deposited on different substrates such as corning glass (Cg), silicon wafer and MgO by PLD technique. All the

substrates induce in-plane strains on the films, but the lattice mismatch between the manganites and the substrate is much larger for MgO than for other substrates. Thin film samples showed a much higher resistance compared to the bulk. For LSMO/MgO the high Curie temperature of 363 K is one of the high  $T_C$  in all LSMO thin films and to the best of our knowledge, it is the highest value that is reported in the literature for MgO substrates with high lattice mismatch parameter. In addition, The Curie temperature of LSMO films is around 352 K, which is one of the high  $T_C$  in all LSMO films and it is the highest value that is reported in literature for low cost amorphous substrates such as glass. The Curie temperature,  $T_c$  is 292 K for LNMO/Cg, 304 K for LNMO/Si and 286K for LNMO/MgO thin films. The relatively high resistance of the polycrystalline thin film may be caused by crack-like defaults and grain boundaries. Magnetoresistance was measured via four point probe technique using Hall effect system. The highest MR value obtained was -17.21% for LSMO/MgO film followed by -15.65% for LSMO/Si film at 80 K in a 1 T magnetic field. Transition temperature ( $T_p$ ) is 224 K for LSMO/MgO and 200 K for LSMO/Si film. The highest MR value obtained was -18.86% for LNMO/MgO film followed by -17.35% for LNMO/Si and 16.59% for LNMO/Cg thin film at 80 K in a 1 T magnetic field. The maximum temperature coefficient of resistance (TCR) ( $10.42\% \text{ K}^{-1}$ ) occurs at  $T = 232 \text{ K}$  for LNMO/MgO film. To our knowledge, this is the best TCR value obtained for LNMO film deposited on the not well-matched MgO substrate. The Curie temperature,  $T_c$  is found from the peak in the  $d\chi'/dT$  via the temperature curve that is 275 K for LSMO/Si, 270 K for LCMO/MgO and 292K for LCMO/Cg thin films. The highest MR value was -24.90% for LCMO/Si thin film, -16.77% for LCMO/Cg and -15.40% for LCMO/MgO thin film at 80 K in a 1 T magnetic field. The phase transition temperature ( $T_p$ ) is 266 K for LCMO/Si,

209K for LCMO/MgO and 231 K for LCMO/Cg thin film. The significant observation in this study is the enhancement of magnetoresistance (MR) up to 36% in the LCMO/ PCMO /LCMO trilayer films. The reason for the enhanced MR suggested that it is due to the induced double exchange mechanism in PCMO by applying the magnetic field. The melting of the charge ordered state is associated with a huge CMR effect.



Abstrak tesis yang dikemukakan kepada Senat Universiti Putra Malaysia sebagai memenuhi keperluan untuk Ijazah Doktor Falsafah

**FABRIKASI DAN PENCIRIAN MAGNETORINTANGAN KOLOSAL  
MANGANIT-MANGANIT DALAM PUKAL, SATU LAPISAN DAN TIGA  
LAPISAN FILEM NIPIS YANG DISEDIAKAN MENGGUNAKAN TEKNIK  
PEMENDAPAN LASER BERDENYUT**

Oleh

**MANIZHEH NAVASERY**

**November 2012**

**Pengerusi: Abdul Halim Shaari, PhD**

**Fakulti: Sains**

Elektronik dan magnet bagi manganit valentoercompur,  $RE_{1-x}M_xMnO_3$  ( $RE$  = nadir bumi,  $M$  = alkali bumi) telah menerima banyak perhatian dalam dekad yang lalu kerana pelbagai fenomena menarik yang dipamerkan oleh bahan-bahan ini. Projek ini bertujuan untuk mengkaji struktur dan sifat magneto-pengangkutan manganite-manganite dalam bentuk pukal, filem nipis tunggal dan tiga lapisan yang disediakan oleh teknik pemendapan Laser berdenyut (PLD) ke atas substrat-substrat yang berbeza. Satu kajian perbandingan antara filem nipis dan pukal dan kesan jenis substrat ke atas struktur, morfologi dan sifat magneto-pengangkutan filem nipis telah dikaji. Selain itu, peningkatan suhu magnetorintangan (MR) dan fasa peralihan ( $T_p$ ) pada filem tiga lapisan turut diselidik. Dalam bahagian pertama polihablur  $La_{2/3}Ca_{1/3} MnO_3$  (LCMO),  $La_{5/8}Sr_{3/8}MnO_3$  (LSMO),  $La_{0.7}Na_{0.3} MnO_3$  (LNMO) dan  $Pr_{0.7}Ca_{0.3} MnO_3$  (PCMO) telah disediakan dengan kaedah

tindak balas keadaan pepejal. Keputusan XRD menunjukkan bahan pukal dan juga filem nipis adalah fasa tunggal dengan struktur ortorombik Pnma bagi LCMO dan PCMO dan struktur rombohedral R $\bar{3}$ C bagi LSMO dan LNMO, dimana tiada bendasing dijumpai. LCMO menunjukkan peralihan logam-penebat pada 274 K, manakala PCMO adalah penebat. Dalam kes LSMO dan LNMO,  $T_p$  adalah di atas suhu bilik. Suhu Curie,  $T_c$ , maganit pukal didapati dari puncak dalam  $d\chi'/dT$  melalui keluk suhu iaitu 94.18K untuk PCMO, 330.42 K untuk LSMO, 319.79 K untuk LNMO dan 285.76 K untuk LCMO. Sampel PCMO berpenebat pada medan magnet sifar, dan mempunyai tertiban caj peralihan sekitar 200 K yang diikuti oleh peralihan antiferromagnet dan feromagnet pada 142.21 K dan 94.18 K yang diperolehi dari bahagian nyata dan khayalan pengukuran kerentenan AC masing. Akhir sekali, pada medan magnet maksimum (10 kG), nilai kemagnetan manganit pukal adalah 46.24 emu/g untuk LSMO, 21.45emu/g untuk LNMO, 5.49 emu/g untuk LCMO dan  $1.66 \times 10^{-3}$  emu/g untuk PCMO. Dalam bahagian kedua kerja ini, manganit  $\text{La}_{2/3}\text{Ca}_{1/8}\text{MnO}_3$  (LCMO),  $\text{La}_{5/8}\text{Ca}_{3/8}\text{MnO}_3$   $\text{La}_{0.3}\text{Na}_{0.7}\text{MnO}_3$  (LNMO) dan  $\text{La}_{5/8}\text{Sr}_{3/8}\text{MnO}_3$  (LSMO) telah dienapkan di atas substrat yang berbeza seperti kaca Corning, wafer silikon dan MgO dengan menggunakan teknik Pemendapan Laser Berdenyut (PLD). Semua substrat mendorong terikan dalam pelan yang luas di atas filem, tetapi ketidakpadanan kekisi di antara manganit-manganit dan substrat adalah lebih besar bagi MgO berbanding substrat lain. Sampel filem nipis menunjukkan rintangan yang lebih tinggi berbanding sampel pukal. Suhu Curie yang tinggi untuk LSMO/MgO iaitu 363 K adalah salah satu  $T_c$  yang tinggi dalam semua filem nipis LSMO dan sebagaimana pengetahuan kami, nilai  $T_c$  ini adalah nilai tertinggi yang dilaporkan dalam kajian literatur untuk substrat MgO dengan

ketidaksepadanan parameter kekisi yang tinggi. Disamping itu, suhu Curie filem LSMO adalah sekitar 352 K, yang merupakan salah satu  $T_C$  yang tinggi dalam semua filem-filem LSMO dan sebagaimana pengetahuan kami, nilai  $T_C$  ini adalah nilai tertinggi yang dilaporkan dalam kajian literatur untuk substrat amorfus kos rendah seperti kaca. Suhu Curie,  $T_c$ , untuk filem-filem nipis LNMO/Cg adalah 292 K, 304 K untuk LNMO/Si dan 286 K untuk LNMO/MgO. Rintangan yang tinggi untuk polihabur filem nipis adalah disebabkan kemungkinan seperti retak dan sempadan butiran. Nilai MR tertinggi diperolehi adalah -17.21% untuk filem LSMO/MgO yang diikuti oleh -15.65% untuk filem LSMO/Si pada 80 K dalam medan magnet 1 T. Suhu peralihan ( $T_P$ ) adalah 224 K untuk LSMO/MgO dan 200 K untuk filem LSMO/Si. Nilai MR tertinggi diperolehi adalah -18.86% untuk filem nipis LNMO/MgO yang diikuti oleh -17.35% untuk LNMO/Si dan 16.59% untuk filem nipis LNMO/Cg pada 80 K dalam medan magnet 1 T. Pekali suhu rintangan maksimum (TCR) ( $10.42\% \text{ } K^{-1}$ ) berlaku pada  $T = 232$  K untuk filem LNMO/MgO. Ini adalah nilai TCR terbaik yang diperolehi bagi filem LNMO yang dienapkan di atas substrat MgO yang tidak sepadan. Suhu Curie,  $T_c$ , filem nipis didapati dari puncak dalam  $d\chi'/dT$  melalui keluk suhu iaitu 275 K untuk LSMO/Si, 270 K untuk LCMO/MgO dan 292 K untuk LCMO / Cg. Nilai MR tertinggi adalah -24.90% untuk filem nipis LCMO/Si, -16.77% untuk filem nipis LCMO/Cg dan -15.40% untuk filem nipis LCMO/MgO pada 80 K dalam medan magnet 1T. Suhu fasa peralihan ( $T_P$ ) bagi filem nipis LCMO/Si adalah 266 K, 209 K untuk LCMO/MgO dan 231 K untuk LCMO/Cg. Pemerhatian penting dalam kajian ini adalah peningkatan magnetorintangan (MR) sehingga 36% dalam filem tiga lapisan LCMO/PCMO/LCMO. Alasan bagi peningkatan MR dicadangkan berpunca dari pengaruhan mekanisme tukarganti berganda dalam PCMO.

dengan menggunakan medan magnet. Kecairan keadaan tertib caj adalah dikaitkan dengan kesan CMR yang besar.



## **ACKNOWLEDGMENT**

The past five years has been a wonderful experience with many ups and downs for me. First and above all, I praise God, the almighty for providing me this opportunity and granting me the capability to proceed successfully. This thesis appears in its current form due to the assistance and guidance of several people. I would therefore like to offer my sincere thanks to all of them. I am extremely grateful to my supervisor, Professor Dr. Abdul Halim Shaari chairman of the supervisory committee for believing in me and for his invaluable advice, guidance, encouragement and continuous discussion. My deepest gratitude goes to my co-supervisors, Dr. Lim Kean Pah, Dr. Chen Soo Kien and Prof. Dr. Roslan Abdul Shukor from Universiti Kebangsaan Malaysia and members of the supervisory.

The assistance provided by the Department of Physics UPM for the use of their X-ray diffraction facility, Institute of Bioscience UPM and ITMA for the use of their FE-SEM facility; is gratefully acknowledged. I am extremely grateful to my lab members and my friends who encourage me at UPM until the end.

Finally, I would like to thank my husband Saeid Goudarzi who has helped me countless times and supported me in all aspects of my life with love. Without his sacrifice and love, I could not come to this point. Thank you indeed my lovely son Danial. I would like to

express great thanks to my family especially my father, my sisters and my brother Hassan for providing me care and love. At last and not at least, I would like to thank my mother in law and sisters in law for their continual support and encouragement.



I certify that a Thesis Examination Committee has met on 5 September 2012 to conduct the final examination of Manizheh Navasery on her thesis entitled "Fabrication and Characterization of Colossal Magnetoresistance Manganites in Bulk, Single layer and Trilayer Thin Films Prepared by Pulsed Laser Deposition Technique" in accordance with the Universities and University College Act 1971 and the Constitution of Universiti Putra Malaysia [P.U.(A) 106] 15 March 1998. The committee recommends that the student be awarded the Doctor of Philosophy.

Members of the Thesis Examination Committee were as follows:

**Azmi bin Zakaria, PhD**

Professor

Faculty of Science

Universiti Putra Malaysia

(Chairman)

**Mansor bin Hashim, PhD**

Associate Professor

Faculty of Science

Universiti Putra Malaysia

(Internal Examiner)

**Jumiah binti Hassan, PhD**

Associate Professor

Faculty of Science

Universiti Putra Malaysia

(Internal Examiner)

**Cheikhrouhou Abdelwahab, PhD**

Professor

Faculty of Science

Sfax-Tunisie

(Independent Examiner)

---

**SEOW HENG FONG, PhD**

Professor and Deputy Dean

School of Graduate Studies

Universiti Putra Malaysia

Date: 22 November 2012

This thesis submitted to the Senate of Universiti Putra Malaysia and has been accepted as fulfilment of the requirements for the degree of Doctor of Philosophy.

The members of the Supervisory Committee were as follows:

**Abdul Halim Shaari, PhD**

Professor

Faculty of Science

Universiti Putra Malaysia

(Chairman)

**Lim Kean Pah, PhD**

Senior Lecturer

Faculty of Science

Universiti Putra Malaysia

(Member)

**Chen Soo Kien, PhD**

Senior Lecturer

Faculty of Science

Universiti Putra Malaysia

(Member)

**Roslan Abd. Shukor, PhD**

Professor

Faculty of Science and Technology

Universiti Kebangsaan Malaysia

(Member)

---

**BUJANG BIN KIM HUAT, PhD**

Professor and Dean

School of Graduate Studies

Universiti Putra Malaysia

Date:

## **DECLARATION**

I declare that the thesis is based on my original work except for quotations and citations, which have been duly acknowledged. I also declare that it has not been previously and is not concurrently, submitted for any other degree at Universiti Putra Malaysia or at any other institutions.

**MANIZHEH NAVASERY**

Date: 22 November 2012

## TABLE OF CONTENTS

	Page
<b>ABSTRACT</b>	iii
<b>ABSTRAK</b>	vi
<b>ACKNOWLEDGMENT</b>	ix
<b>APPROVAL</b>	x
<b>DECLARATION</b>	xii
<b>LIST OF TABLES</b>	xviii
<b>LIST OF FIGURES</b>	xx
<b>LIST OF ABBREVIATIONS /NOTATIONS/GLOSSARY OF TERMS</b>	xxix
<b>CHAPTER</b>	
<b>1. INTRODUCTION</b>	1
1.1 General Introduction	1
1.2 Applications of CMR materials	3
1.3 Problem Statement	5
1.4 Objective of Thesis	7
1.5 Plan of Thesis	7
<b>2. LITERATURE REVIEW</b>	9
2.1 Introduction	9
2.2 Discovery of Colossal Magnetoresistance (CMR) effect	10
2.3 Mixed-Valence Perovskites of $\text{RE}_{1-x}\text{M}_x\text{MnO}_3$	12
2.3.1 Effects of A-site Cation Size	13
2.3.2 Effects of Doping Level	16
2.3.2.1 $\text{La}_{1-x}\text{Ca}_x\text{MnO}_3$ (LCMO) Manganites	16
2.3.2.2 $\text{La}_{1-x}\text{Sr}_x\text{MnO}_3$ (LSMO) Manganites	22
2.3.2.3 $\text{La}_{1-x}\text{Na}_x\text{MnO}_3$ (LNMO) Manganites	27
2.4 Multilayer Manganite Films	32

<b>3. THEORY</b>	35
3.1 Introduction	35
3.2 Magnetoresistance	36
3.3 Colossal Magnetoresistance (CMR)	37
3.3.1 Type of Magnetoresistance	38
3.3.2 Transport and Magnetotransport	39
3.3.2.1 Conduction Mechanism	41
3.4 Crystal Structure of the Manganites	44
3.5 Phase Diagram of Manganites	46
3.5.1 $\text{La}_{1-x}\text{Ca}_x\text{MnO}_3$	46
3.5.2 $\text{La}_{1-x}\text{Sr}_x\text{MnO}_3$	49
3.5.3 $\text{Pr}_{1-x}\text{Ca}_x\text{MnO}_3$	50
3.6 Exchange Interaction	51
3.6.1 Superexchange	51
3.6.2 Double Exchange	52
3.7 The Jahn-Teller Effect	55
3.8 Fundamental of Pulsed Laser Deposition	58
3.8.1 Mechanism of Pulsed Laser Deposition (PLD)	59
3.8.1.1 Laser-Target Interaction	59
3.8.1.2 Plasma Plume Formation	61
3.8.1.3 Nucleation and Growth of Thin Films	62
3.8.2 Deposition Parameters	65
3.8.2.1 Laser power density	65
3.8.2.2 Repetition rate (time between laser pulses) and pulse duration	66
3.8.2.3 Substrate Temperature	69
3.8.2.4 Background gas pressure	69
3.8.2.5 Distance between target and substrate	71
3.8.3 The advantages and disadvantages of PLD	72
<b>4. MATERIALS AND METHODS</b>	75
4.1 Sample Preparation	75
4.1.1 Polycrystalline (Bulk) Samples	75

4.1.1.1	Weighing and Mixing	76
4.1.1.2	Calcination	77
4.1.1.3	Grinding and pelletizing	77
4.1.1.4	Sintering	78
4.1.2	Thin film Samples	80
4.1.2.1	The PLD Setup	80
4.1.2.2	Thin film growth	81
4.2	Sample characterization	85
4.2.1	X-Ray Diffraction (XRD)	87
4.2.2	Microstructure Characterization	88
4.2.2.1	Field-Emission Scanning Electron Microscope (FE-SEM)	88
4.2.2.2	Atomic Force Microscope (AFM)	90
4.2.3	Magnetic Characterization	92
4.2.3.1	AC Magnetic Susceptibility	92
4.2.3.2	Magnetoresistance (MR)	95
4.2.3.3	Vibrating Sample Magnetometer (VSM)	96
4.2.4	Electrical-Resistance Measurement	97
4.2.5	Film Thickness Measurement	98
4.2.6	Accuracy of Measurement	99
<b>5.</b>	<b>RESULT AND DISCUSSION</b>	100
5.1	Polycrystalline Bulk Colossal Magnetoresistance (CMR)	101
5.1.1	XRD analysis and Rietveld's Refinement	101
5.1.1.1	$\text{La}_{2/3}\text{Ca}_{1/3}\text{MnO}_3$ and $\text{La}_{5/8}\text{Sr}_{3/8}\text{MnO}_3$	101
5.1.1.2	$\text{La}_{0.7}\text{Na}_{0.3}\text{MnO}_3$ system	104
5.1.1.3	$\text{Pr}_{0.7}\text{Ca}_{0.3}\text{MnO}_3$ system	106
5.1.2	Microstructure Analysis	109
5.1.3	AC Magnetic Susceptibility and Curie temperature Measurement	113
5.1.4	Colossal Magnetoresistance Effect (CMR)	117
5.1.5	Magnetization and Hysteresis Loop	124
5.1.6	Electric Resistance and Phase Transition	125
5.2	Single Layer Thin Films	132

5.2.1	Single Layer Thin Film of $\text{La}_{5/8}\text{Sr}_{3/8}\text{MnO}_3$ (LSMO) growth on MgO (100) and Si (100) substrates	132
5.2.1.1	XRD analysis and Rietveld's Refinement	132
5.2.1.2	Microstructure Analysis	136
5.2.1.3	AC Magnetic Susceptibility and Curie temperature Measurement	138
5.2.1.4	Colossal Magnetoresistance Effect (CMR)	141
5.2.1.5	Electric Resistance Measurement	143
5.2.2	Single Layer Thin Film of $\text{La}_{5/8}\text{Sr}_{3/8}\text{MnO}_3$ (LSMO) growth on glass	156
5.2.2.1	XRD analysis and Rietveld's Refinement	156
5.2.2.2	Microstructure Analysis	160
5.2.2.3	AC Magnetic Susceptibility and Curie temperature Measurement	164
5.2.2.4	Colossal Magnetoresistance Effect (CMR)	164
5.2.2.5	Electric Resistance and Phase Transition	167
5.2.3	Single Layer Thin Film of $\text{La}_{0.7}\text{Na}_{0.3}\text{MnO}_3$	171
5.2.3.1	XRD analysis and Rietveld's Refinement	171
5.2.3.2	Microstructure Analysis	176
5.2.3.3	AC Magnetic Susceptibility and Curie temperature Measurement	180
5.2.3.4	Colossal Magnetoresistance Effect (CMR)	180
5.2.3.5	Electric Resistance Measurement	184
5.2.4	Single Layer Thin Film of $\text{La}_{2/3}\text{Ca}_{1/3}\text{MnO}_3$ (LCMO)	203
5.2.4.1	XRD analysis and Rietveld's Refinement	203
5.2.4.2	Microstructure Analysis	207
5.2.4.3	AC Magnetic Susceptibility and Curie temperature Measurement	214
5.2.4.4	Colossal Magnetoresistance Effect (CMR)	216
5.2.4.5	Electric Resistance Measurement	218
5.3	Trilayer Manganite Films	233
5.3.1	XRD analysis and Rietveld's Refinement	233
5.3.2	Microstructure Analysis	239

5.3.3	Electric Resistance and Phase Transition	243
5.3.4	Colossal Magnetoresistance Effect (CMR)	253
<b>6.</b>	<b>CONCLUSION</b>	<b>258</b>
6.1	Conclusions	258
6.1.1	Polycrystalline bulk Colossal Magnetoresistance (CMR)	258
6.1.2	Single Layer Thin Films	260
6.1.2.1	Single Layer Thin Film of $\text{La}_{5/8}\text{Sr}_{3/8}\text{MnO}_3$ (LSMO) growth on $\text{MgO}$ (100) and $\text{Si}$ (100) substrates	260
6.1.2.2	Single Layer Thin Film of $\text{La}_{5/8}\text{Sr}_{3/8}\text{MnO}_3$ (LSMO) growth on glass	261
6.1.2.3	Single Layer Thin Film of $\text{La}_{0.7}\text{Na}_{0.3}\text{MnO}_3$	262
6.1.2.4	Single Layer Thin Film of $\text{La}_{2/3}\text{Ca}_{1/3}\text{MnO}_3$ (LCMO)	264
6.1.3	Trilayer Manganite Films	265
6.2	Recommendation for Future Work	267
<b>REFERENCES</b>		<b>269</b>
<b>BIODATA OF STUDENT</b>		<b>281</b>
<b>PUBLICATION</b>		<b>282</b>

## LIST OF FIGURES

Figure	Page
1.1 Normalized resistance via temperature for superconductor (YBCO) and manganite (LCMO) at zero magnetic field	5
2.1 Three magnetoresistance versus temperature curves for different	11
2.2 Phase diagram of temperature versus tolerance factor and average radius of cation at A site for the system $\text{RE}_{0.7}\text{A}_{0.3}\text{MnO}_3$	14
2.3 Two-dimensional schematic drawing of two perovskite (for $N_A=2$ and $N_A=3$ )	15
2.4 The transport properties of the 10h-milled samples with different heat-treated temperatures	18
2.5 The R-T curves of LCMO as deposited films A( $650^\circ\text{C}$ ), B( $700^\circ\text{C}$ ) and post-annealed film A'( $650^\circ\text{C}$ ), B'( $700^\circ\text{C}$ )	22
2.6 Resistivity against $T$ for $\text{La}_{1-x}\text{Sr}_x\text{MnO}_3$ for various $x$ values. The arrows denote the transition as determined by magnetization measurements	23
2.7 AFM images of the samples (a) LSMO600 ( $P_{\text{O}_2}=10^{-2}$ mbar), (b) LSMO700 ( $P_{\text{O}_2}=10^{-2}$ mbar), (c) LSMO800( $P_{\text{O}_2}=10^{-2}$ mbar) and (d) LSMO700( $P_{\text{O}_2}=1^2$ mbar)	25
2.8 SEM observation of typical LSMO films with regular spare pattern of 40 nm size grain nano-structure on $\text{SrTiO}_3$	26
2.9 Electrical resistivity vs. temperature of Na-doped manganite at different sintering temperatures	29
2.10 The AFM images of the sample $\text{Na}(x=0.1)$ , $\text{Na}(x=0.15)$ and $a(x=0.3)$ , respectively	31
2.11 Resistance as a function of temperature for a LSMO/L0.75MO (70 nm)/LSMO trilayer film. The results of LSMO and L0.75MO single layer films are also shown for comparison	33
3.1 CMR behavior for the $\text{La}_{0.67}\text{Ca}_{0.33}\text{MnO}_3$ single crystal	38
3.2 (a) Perovskite structure of manganites , (b) 3-D Network of $\text{MnO}_6$ octahedra surrounding $\text{R}_A$ ion in the perovskite structure, (c) Distortion of a perovskite structure	45

3.3	(a) The phase diagram of $\text{La}_{1-x}\text{Ca}_x\text{MnO}_3$ , (b) The charge and orbital ordering for $\text{La}_{1-x}\text{Ca}_x\text{MnO}_3$ with $x=0$ , $1/2$ , $1/3$ and $2/3$	48
3.4	Phase diagrams of single crystals of $\text{La}_{1-x}\text{Sr}_x\text{MnO}_3$ and $\text{Pr}_{1-x}\text{Ca}_x\text{MnO}_3$	51
3.5	Schematic illustrations of (a) superexchange, (b) double exchange in manganites	54
3.6	Jahn-Teller effect in manganites	56
3.7	Cooperative JT distortions and resulting lattice	57
3.8	A phase diagram study of the local structure of the colossal magnetoresistant manganite material $\text{La}_{1-x}\text{Ca}_x\text{MnO}_3$ . The color scale is the height of a PDF peak that is sensitive to the presence (blue) or absence (red) of a local Jahn-Teller distortion	57
3.9	Schematic of a pulsed laser deposition system using in this work	58
3.10	Schematic of thermal cycle during a laser strike on the target (a) absorption of the laser radiation, (b) propagation of melt front and evaporation of material, (c) recoil of thermal shockwave and (d) solidification of the surface	61
3.11	Illustrations of the basic growth modes including (a) Volmer–Weber (island), (b) Frank–Van der Merwe (layer-by-layer), and (c) Stranski–Krastanov (island and layer-by-layer) growth	64
3.12	ICCD images of laser-induced plasma at different delay times and laser pulse fluences (titanium target; the 1064 nm laser pulse starts at $t=0$ and completes at $t=200$ ns; laser beam propagates downwards and the target surface is located at the bottom of the images)	67
3.13	(Color online) Contour plots of normalized radiation intensity distribution for laser-induced plasma at different delay times and laser pulse fluences (titanium target; laser parameters are the same as Figure 3.12 the horizontal and vertical coordinates are in micron)	68
3.14	Time ICCD-images of laser plume expanding of YBCO superconductor, into vacuum (a-f) and 100 mTorr $\text{O}_2$ (g-l)	71
4.1	Simple view of sintering process in solid state reaction route	78
4.2	The basic of solid state process for fabrication of targets	79

4.3	Schematic of the PLD setup used for this work	81
4.4	Schematic diagram of four point probe resistance measurement	83
4.5	Schematic diagram of our system during the deposition	84
4.6	The overall experimental procedures for all samples in this work	86
4.7	FE-SEM image of cross-section of LSMO trilayers (taken from my research work at UPM)	89
4.8	3D and 2D AFM micrographs of the deposited LNMO thin films on MgO(100)	91
4.9	Schematic view of CryoBIND T AC Susceptometer of coil system	94
4.10	Schematic diagram of Magnetoresistance (MR) measurement by Hall Measurement System using four- point probe technique	95
4.11	( a) Schematic diagram of VSM (b) M-H curve (hysteresis loops) of FM and SPM materials; the in the corner shows the direction of external magnetic field	97
4.12	Schematic diagram of four point probe resistance measurement	98
5.1	(a) XRD patterns of the LCMO and LSMO bulk samples (b) The main peaks of the XRD patterns for LCMO and LSMO bulk samples	103
5.2	Structure of LCMO bulk, showing MnO <sub>6</sub> octahedra and distortions of the Mn-O-Mn angles from 180°	104
5.3	XRD patterns of the LNMO bulk sample	105
5.4	X-ray diffraction patterns of PCMO sample	107
5.5	The Reitveld refined graphs for PCMO sample. The below pattern shows the difference between the observed and calculated patterns	107
5.6	FE-SEM micrographs of LCMO, LSMO and LNMO bulk samples with magnification of 2KX and 5KX	111
5.7	(a) The top view of PCMO target before and after laser ablation (b) SEM image of PCMO target before laser ablation (c) SEM image of laser ablated ring on surface of PCMO target with magnification of 2KX and 5KX	112
5.8	Distribution of grains of (a) LCMO, (b) PCMO, Cc)LNMO and (d) LSMO bulk manganites	113

5.9	The temperature dependence of real part of ac susceptibility for (a) PCMO. (b) LSMO, (c) LNMO and (d) LCMO bulk samples in ac field amplitude of 1 Oe	115
5.10	Derivatives of the AC susceptibility ( $d\chi'/dT$ ) vs. temperature for (a) PCMO, (b) LSMO, (c) LNMO and (d) LCMO bulk samples	116
5.11	Normalized imaginary curve of AC susceptibility versus temperature for PCMO sample. (FMI: Ferromagnetic Insulator; AFM: Antiferromagnetic (insulator); COI: Charge-Ordering Insulator; $T_{CA}$ : Canted ferromagnetic transition temperature; $T_N$ : N'eel Temperature)	117
5.12	(a) %MR curve of LCMO bulk as function of magnetic field at various temperatures (b) The temperature dependence of %MR curve for LCMO bulk sample	120
5.13	(a) %MR curve of LSMO bulk as function of magnetic field at various temperatures (b) The temperature dependence of %MR curve for LSMO bulk sample	121
5.14	(a) %MR curve of LNMO bulk as function of magnetic field at various temperatures (b) The temperature dependence of %MR curve for LNMO bulk sample	122
5.15	(a) Temperature dependence of resistance for PCMO bulk sample at 0T and 1T magnetic field (b) %MR versus temperature curve for LNMO bulk sample from 100 to 300 k	123
5.16	Magnetic field dependence of magnetization at 300 K for LSMO, LNMO, LCMO and PCMO bulk manganite samples at 10 KG	125
5.17	Temperature dependence of normalized resistance at zero magnetic field for PCMO, LSMO, LNMO and LCMO bulk manganites	128
5.18	Temperature dependence of resistance at zero magnetic field for LCMO bulk manganite; FMI: Ferromagnetic Insulator, PMI: Paramagnetic Insulator, FMM: Ferromagnetic Metal	129
5.19	(a) Temperature dependence of resistance at zero magnetic field for PCMO bulk manganite, (b) Temperature dependence of $d(\ln R)/d(1/T)$ indicating $T_{CO}$ ; PMI: Paramagnetic Insulator, CO: Charge-Ordering (insulator)	130
5.20	Temperature dependence of %TCR for PCMO, LSMO, LNMO and LCMO bulk samples	131

5.21	XRD patterns of the LSMO films deposited on MgO(100) and Silicon(100) wafer substrates	134
5.22	A typical plot of XRD pattern of LSMO/Si sample along with Rietveld refined pattern. The second pattern shows the difference between the observed and calculated patterns	134
5.23	FE-SEM micrographs of LSMO/Si and LSMO/MgO thin films with magnification of 1 KX, 50 KX	137
5.24	Distribution of grains of LSMO/MgO and LSMO/Si thin films	138
5.25	Temperature dependence of real part of AC susceptibility for LSMO/MgO and LSMO/Si thin films in AC field amplitude of 1 Oe	140
5.26	%MR curve of LSMO /Si and LSMO/MgO thin films as function of magnetic field at various temperatures	142
5.27	Temperature dependence of normalized resistance at zero magnetic field for all manganite thin films	144
5.28	$\ln \rho$ versus temperature for LSMO films below $T_p$ . The solid line representing the best fit to Equation(3.4)	147
5.29	Inverse temperature dependence of $\ln(\rho/T)$ above $T_p$ for (a) LSMO/Si and (b) LSMO/MgO thin films by using of SPH model	149
5.30	$\ln(\rho/T)$ and $\ln(\rho/T^{1.5})$ versus $(1/T)$ plot for LSMO/Si thin films above $\theta_D/2$ (266 K) (a) for SPH-Adiabatic model (b) for SPH(Non-Adiabatic) model	150
5.31	$\ln(\rho/T)$ and $\ln(\rho/T^{1.5})$ versus $(1/T)$ plot for LSMO/MgO thin films above $\theta_D/2$ (272 K) (a) for SPH-Adiabatic model (b) for SPH(Non-Adiabatic) model	151
5.32	$\ln(\rho)$ versus $T^{-1/4}$ for (a) LSMO/Si and (b) LSMO/MgO thin films at best fitting temperature range of VRH model. Lines represent the results for fitting 3D-VRH models	155
5.33	Room temperature XRD patterns of LSMO bulk and thin film	158
5.34	Rietveld analysis of XRD data for LSMO/Cg thin film	158
5.35	FE-SEM images and distribution of grain size of LSMO thin film	162

5.36	(a) 3D-AFM micrography of the deposited LSMO film on glass wiyh scan area of $20 \mu\text{m} \times 20 \mu\text{m}$ ; (b) 2D- AFM micrography and surface cross section of the of the deposited LSMO film on glass	163
5.37	(a). Temperature dependence of real part of ac susceptibility for LSMO/Cg thin film in AC field amplitude of 1 Oe and frequency of 240 Hz; (b) T <sub>c</sub> is found from the peak in the $d\chi'/dT$ via temperature curve or from inverse of susceptibility via temperature curve, where the linear fit gives a Curie temperature	165
5.38	%MR curve of LSMO /Cg film as function of magnetic field at various temperatures	166
5.39	Normalized temperature dependence of the LSMO film and bulk in zero magnetic fields in the temperature range of 100–300 K	169
5.40	Resistivity vs. absolute temperature curve for LSMO /Cg thin film below T <sub>p</sub> ; the solid line gives the best fit to Equation (3.4)	170
5.41	(a) XRD patterns of the LNMO/MgO, LNMO/Cg and LNMO/Si thin films (b) The main peaks of the XRD patterns for LNMO thin films	174
5.42	A typical plot of XRD pattern of LNMO/Si sample along with Rietveld refined pattern. The second pattern shows the difference between the observed and calculated patterns. The remain diffraction peak comes from the Si (100) substrate	176
5.43	FE-SEM micrographs of LNMO/Cg, LNMO/Si and LNMO/MgO thin films with magnification of 1 KX and 25 KX	178
5.44	FE-SEM micrographs of LNMO/Cg thin film with magnification of 1KX and 5 KX	179
5.45	Distribution of grains of LNMO thin films	179
5.46	(a) Temperature dependence of real part of AC susceptibility for LNMO thin films in ac field amplitude of 1 Oe. (b) Derivatives of the AC susceptibility ( $d\chi'/dT$ ) vs. temperature of LNMO thin films	181
5.47	%MR curve of LSMO /Si and LSMO/MgO thin films as function of magnetic field at various temperatures	183
5.48	Temperature dependence of normalized resistance at zero magnetic field for all LNMO manganite thin films	186

5.49	Temperature dependence of %TCR for LNMO film deposited on MgO (100) substrate	187
5.50	$\ln \rho$ versus temperature for (a) LNMO/Cg, (b) LNMO/Si and (c) LNMO/MgO thin films below $T_p$ . The solid line represents the best fit to Equation(3.4)	190
5.51	Inverse temperature dependence of $\ln(\rho/T)$ above $T_p$ for (a) LNMO/Cg, (b) LNMO /Si and (c) LNMO/MgO thin films by using of SPH model	193
5.52	$\ln(\rho/T)$ and $\ln(\rho/T^{1.5})$ versus $(1/T)$ plot for LNMO/Cg thin films above $\theta_D/2$ (272 K) (a) for SPH–Adiabatic model (b) for SPH(Non-Adiabatic) model	194
5.53	$\ln(\rho/T)$ and $\ln(\rho/T^{1.5})$ versus $(1/T)$ plot for LNMO/Si thin films above $\theta_D/2$ (274 K) (a) for SPH–Adiabatic model (b) for SPH(Non-Adiabatic) model	195
5.54	$\ln(\rho/T)$ and $\ln(\rho/T^{1.5})$ versus $(1/T)$ plot for LNMO/MgO thin films above $\theta_D/2$ (244 K) (a) for SPH–Adiabatic model (b) for SPH(Non-Adiabatic) model	196
5.55	(a) $\ln(\rho)$ versus $T^{-1/4}$ (b) $\ln(\rho)$ versus $T^{-1/3}$ for LNMO/Cg thin film at best fitting temperature range of VRH model. Lines represent the results for fitting VRH models	200
5.56	(a) $\ln(\rho)$ versus $T^{-1/4}$ (b) $\ln(\rho)$ versus $T^{-1/3}$ for LNMO/Si thin film at best fitting temperature range of VRH model. Lines represent the results for fitting VRH models	201
5.57	(a) $\ln(\rho)$ versus $T^{-1/4}$ (b) $\ln(\rho)$ versus $T^{-1/3}$ for LNMO/MgO thin film at best fitting temperature range of VRH model. Lines represent the results for fitting VRH models	202
5.58	(a)The XRD patterns of the LCMO/Si (LS), LCMO/Cg (LC) and LCMO/MgO (LM) thin films (b) the main peaks of the XRD patterns for LS, LC and LM thin films	205
5.59	FE-SEM micrographs of LCMO/Cg, LNMO/Si and LNMO/MgO thin films with magnification of 5 KX and 100 KX	209
5.60	Grain size distribution of (a) LCMO/Si, (b) LCMO/Cg and (c) LCMO/MgO thin films	210
5.61	FE-SEM images of (a) the surface and (b) cross-sectional morphologies of the LCMO/Si thin film	211

5.62	3D and 2D - AFM micrographs of the deposited LCMO thin films on Si(100), MgO(100) and glass substrates in scan area of $20 \mu\text{m} \times 20 \mu\text{m}$	212
5.63	(a) 2D- AFM micrographes and surface cross section of the of the deposited LCMO film on Si(100), MgO(100) and glass substrates; (b) 2D-AFM image of LCMO/Cg indicating the island-growth of film	213
5.64	(a). The temperature dependence of real part of AC susceptibility for (a) LCMO/Si, (b) LCMO/MgO and (c) LCMO/Cg thin films in ac field amplitude of 1 Oe. (d) Derivatives of the AC susceptibility ( $d\chi'/dT$ ) vs. temperature of LCMO/Si thin film	215
5.65	%MR curve of (a) LCMO /Si, (b) LCMO/Cg and (c) LCMO/MgO thin films as function of magnetic field at various temperatures	217
5.66	Temperature dependence of normalized resistance at zero magnetic field for all manganite thin films	219
5.67	$\ln \rho$ versus temperature for (a) LNMO/Cg, (b) LNMO/Si and (c) LNMO/ MgO thin films below $T_p$ . The solid line representing the best fit to Equation (3.4)	222
5.68	Inverse temperature dependence of $\ln(\rho/T)$ above $T_p$ for (a) LCMO/Si, (b)LCMO/MgO and (c) LCMO/Cg thin films by using of SPH model	224
5.69	$\ln(\rho/T)$ and $\ln(\rho/T^{1.5})$ versus $(1/T)$ plot for LCMO/Si thin films above $\theta_D/2$ (284 K) (a) for SPH–Adiabatic model (b) for SPH(Non-Adiabatic) model	225
5.70	$\ln(\rho/T)$ and $\ln(\rho/T^{1.5})$ versus $(1/T)$ plot for LCMO/MgO thin films above $\theta_D/2$ (254 K) (a) for SPH–Adiabatic model (b) for SPH(Non-Adiabatic) model	226
5.71	$\ln(\rho/T)$ and $\ln(\rho/T^{1.5})$ versus $(1/T)$ plot for LCMO/Cg thin films above $\theta_D/2$ (274 K) (a) for SPH–Adiabatic model (b) for SPH(Non-Adiabatic) model	227
5.72	$\ln(\rho)$ versus $(T^{-1/4})$ and $(T^{-1/3})$ at temperature rangeof $266 \text{ K} < T < 284 \text{ K}$ for LCMO/Si thin film. The red colour lines represent the result for fitting by 3D-VRHand 2D-VRH models	230
5.73	$\ln(\rho)$ versus $(T^{-1/4})$ and $(T^{-1/3})$ at temperature range of $209 \text{ K} < T < 254 \text{ K}$ for LCMO/MgO thin film. The red colour lines represent the result for fitting by 3D-VRHand 2D-VRH models	231

5.74	$\text{Ln}(\rho)$ versus $(T^{-1/4})$ and $(T^{-1/3})$ at temperature range of $231 \text{ K} < T < 274 \text{ K}$ for LCMO/Cg thin film. The red colour lines represent the result for fitting by 3D-VRHand 2D-VRH models	232
5.75	(a) XRD patterns of the LCMO single and trilayer with two different PCMO space layer thickness ; (b) The peaks of the silicon wafer substrate	235
5.76	FE-SEM images of the top view for LCMO single layer (LC-1th) and LCMO trilayer (LP <sub>1</sub> L) in magnification of 5 XK, 50 XK, 100 K and 200 XK	239
5.77	FE-SEM image of cross section of LCMO trilayer (LP <sub>1</sub> L) thin film ; in left image the layers can be observed separately	240
5.78	Distribution of grains of (a) LCMO –Single layer thin film (b) LCMO-Trilayer(LP <sub>1</sub> L) thin film.	241
5.79	FE-SEM images of the top view for LCMO single layer (LC-1th) and LCMO trilayers (LP <sub>2</sub> L) in magnification of 5 XK, 25 XK, 50 XK and 100 XK	241
5.80	FE-SEM image of cross section of LCMO trilayer (LP <sub>2</sub> L) (a) LCMO (1st) first layer (b) LCMO (3rd) top layer	242
5.81	(a)Temperature dependence of resistance for LP <sub>1</sub> L trilayer (for LCMO-first layer) at 0 T and 1 T magnetic field (b) View of fore point probe set up for R(T) measurements	246
5.82	(a) Temperature dependence of resistance for LP <sub>1</sub> L trilayer (for LCMO-top layer) at 0 T and 1 T magnetic field (b) View of fore point probe set up for R (T) measurements	247
5.83	(a) Temperature dependence of resistance for LP <sub>1</sub> L trilayer at 0 T and 1 T magnetic field (b) View of fore point probe set up for R(T) measurements	248
5.84	Temperature dependence of resistivity for LP <sub>1</sub> L trilayer (for LCMO-firs layer and LCMO-top layer) at 0 T magnetic field	249
5.85	Temperature dependence of resistivity for PCMO (bulk) sample and PCMO/LCMO bilayer at 1 T magnetic field (b) View of fore point probe set up for $\rho(T)$ measurements (for PCMO/LCMO bilayer)	251
5.86	Temperature dependence of resistance for LP <sub>2</sub> L at 0 T and 1 T magnetic field (b) View of fore point probe set up for R(T) measurements	251

5.87	Temperature dependence of resistance for LP <sub>2</sub> L (for LCMO-top layer) at 0T and 1 T magnetic field (b) View of fore point probe set up for R(T) measurements	252
5.88	Temperature dependence of resistivity for LP <sub>2</sub> L trilayer (for LCMO-firs layer and LCMO-top layer) at 0T magnetic field	253
5.89	Temperature dependence of %MR curve for (a) LP <sub>1</sub> L trilayer	256
5.90	Temperature dependence of %MR curve for (a) LCMO (top layer); (b) LCMO (based layer)	257



## LIST OF ABREVIATIONS /NOTATIONS/GLOSSARY OF TERMS

AFM	Antiferromagnetic, Atomic Force Microscopy
AFI	Antiferromagnetic Insulating
CMR	Colossal Magnetoresistance
CE	Charge Exchange
CO	Charge Ordering
CAF	Canted Antiferromagnetic
DE	Double Exchange Mechanism
FWHM	Full Width Half Maximum
GB	Grain Boundary
GMR	Giant Magnetoresistance
RE	Rare Earth element
PM	Paramagnetic
PLD	Pulsed Laser Deposition
MR	Magnetoresistance
FE-SEM	Field Emission- Scanning Electron Microscope
VSM	Vibration Sample Magnetometer
LAO	$\text{LaAlO}_3$
JT	Jahn-Teller distortion
$T_p$	Phase Transition Temperature
$T_c$	Curie temperature

$T_N$	Neel Temperature
FMI	Ferromagnetic Insulator
FMM	Ferromagnetic Metallic
LSMO	$\text{La}_{1-x}\text{Sr}_x\text{MnO}_3$ , $\text{La}_{5/8}\text{Sr}_{3/8}\text{MnO}_3$
LNMO	$\text{La}_{1-x}\text{Na}_x\text{MnO}_3$ , $\text{La}_{0.7}\text{Na}_{0.3}\text{MnO}_3$
LCMO	$\text{La}_{1-x}\text{Ca}_x\text{MnO}_3$ , $\text{La}_{2/3}\text{Ca}_{1/3}\text{MnO}_3$
PCMO	$\text{Pr}_{1-x}\text{Ca}_x\text{MnO}_3$ , $\text{Pr}_{0.7}\text{Ca}_{0.3}\text{MnO}_3$
$T_{MI}$	Metal-Insulator Temperature
STO	$\text{SrTiO}_3$
XPD	X-ray Diffraction
AMR	Anisotropic magnetoresistance
TMR	Tunnelling magnetoresistance
Cg	Corning glass

# CHAPTER ONE

## INTRODUCTION

### 1.1 General Introduction

In the last 20 years, two classes of materials have defined and dominated the landscape of condensed matter physics study of oxide materials: high-temperature superconductivity in doped cuprates and doped manganites. Figure 1.1 typically shows Normalized resistance via temperature for superconductor (YBCO) and manganite (LCMO) at zero magnetic field. The research in the field of spintronics contents phenomena such as giant magnetoresistance (GMR), colossal magnetoresistance (CMR), spin-tunneling in junctions (STJ), spin coherence and spin dephasing have attracted more attention. The spintronics (Daughton et al., 1999; Gregg et al., 2002; Wolf et al., 2001; Žutić et al., 2004) is defined as the branch of electronics that utilizes the spin degree of freedom of the electron together with its charge, to store and transmit information. The discovery of negative magnetoresistance (MR) in rare-earth manganates,  $RE_{1-x}A_xMnO_3$  ( $RE$  = rare earth,  $A$  = alkaline earth) with the perovskite structure, has attracted wide attention. The magnitude of MR in these materials can be very large, more than of 100%. For this reason, many workers prefer to call this colossal magnetoresistance (CMR), as distinct from gaint magnetoresistance (GMR) in layered

or granular metallic materials. In metallic multilayers or granular alloys, the mechanism involves spin-polarized transport. In the manganates also, spinpolarized transport is responsible for the large negative MR, but it is distinctly different from what happens in the metallic multilayers.

The properties of manganites compounds with a  $Mn^{3+}/Mn^{4+}$  mixed valence keep attracting attention from both experimentalists and theorists. The rich phase diagram with entangled insulating, metallic, ferromagnetic (FM), antiferromagnetic (AFM) and paramagnetic phases, reveals a strong coupling between the lattice, spin and electronic degrees of freedom. These called double exchange mechanism assuming the oxygen mediated electron exchange between neighboring  $Mn^{3+}/Mn^{4+}$  sites is only a starting point of modelling (Haghiri-Gosnet and Renard, 2003). The mobility of the conduction electron between  $Mn^{3+}/Mn^{4+}$  pairs is greatly enhanced when the magnetic moments on adjacent Mn ions are aligned. The mixed valence also leads to the formation of small polarons, arising from  $Mn^{3+}/Mn^{4+}$  valence changes and to Jahn-teller distortion involving Mn that leads to incoherent hopping and high resistivity in the insulating phase. The  $Mn^{3+}$ - $O^{2-}$ - $Mn^{4+}$  bond lengths and angles play a crucial role in determining the magnetotransport in manganites (Teplykh et al., 2004). Moreover, an applied magnetic field enhances the FM order, thus reduces the spin scattering and produces a so-called negative colossal magnetoresistance (CMR) peak.

## 1.2 Applications of CMR materials

The manganite materials are especially interesting since they present large electronic correlations leading to a strong competition between lattice, charge, spin, and orbital degrees of freedom. These manganese-based perovskite oxides exhibit half-metallic character and CMR response rendering them as the ideal materials to develop novel concepts of oxide-electronic devices and for the study of fundamental physical interactions. Due to the close similarity between kinetic energy of charge carriers and Coulomb repulsion, tiny perturbations caused by small changes in temperature, magnetic or electric fields, strain and so forth may drastically modify the magnetic and transport properties of these materials. In addition, the half metallic character may find applications in spintronics. The simplest type of application is the spin-valve device: an insulating tunnel barrier is sandwiched between magnetic metal. Due to the high spin-polarization of carriers in half-metallic manganites, the spin dependent tunneling between two ferromagnetic manganites electrodes across a thin insulating barrier should produce a large magneto-resistance response.

Moreover, because these materials should allow true on-of operations, they would be very appropriate for sensor elements of non-volatile devices. Unfortunately, the CMR effect currently requires very high magnetic fields and low temperatures for most materials making them impractical for use in devices. Therefore, currently, high magnetoresistance at room temperature and under low magnetic field are more

interested. Magnetoresistance (MR) is important in many technological applications, such as magnetic data storage, read - write heads, magnetic - bolometric sensors, magnetic tunnel junction (MTJ) and magnetoresistive random access memory (MRAM).

In summary, few applications of CMR materials are listed below:

1. Magnetic field sensors

- (a) Using the CMR effect in a film
- (b) Using a spin valve structure
- (c) As a microwave CMR sensor

2. Electric field effect devices

- (a) Using a  $\text{SrTiO}_3$  gate
- (b) Using a ferroelectric gate

3. Bolometric uncooled infrared (IR) sensors using the metal -insulator transition at Curie temperature

4. Low temperature hybrid HTS-CMR devices

- (a) Flux focused magnetic transducers
- (b) Spin polarized quasi-particle injection devices

The industrial requirements for a magnetic sensor can be summarized as follows.

1. Operation at room temperature and up to 100 K above room temperature.

2. At least a 20% response at a field of 100 Gauss

3. Temperature independent CMR values over 50-350 K

4. Acceptable noise values

5. Retention of magneto-transport properties in patterned films at dimensions

approaching sub-1000Å scales. (The current thinking is that oxide-based CMR sensors will have maximum impact only on memory systems approaching densities of 100 Gb/cm<sup>2</sup>).

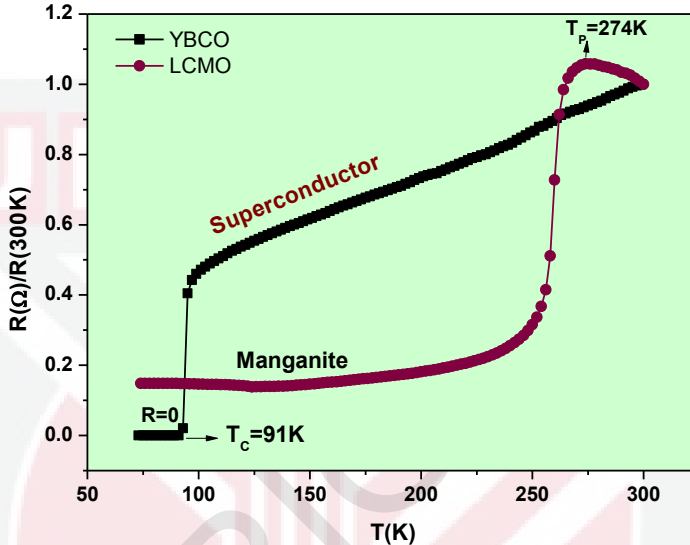


**Figure 1.1:** Normalized resistance via temperature for superconductor (YBCO) and manganite (LCMO) at zero magnetic field (The results are taken from my research work at UPM).

### 1.3 Problem Statement

Currently manganite research is one of the research topics in solid state condensed matter physics, aiming to improve the understanding of the behavior of electrons in crystals. There are two main reasons interesting to the manganites as background of this

study. The first reason is the unexpectedly large magnetotransport properties of these materials. By application of relatively small magnetic fields, the resistivity changes by several orders of magnitude. A second motivation to study the manganites is contained in their rich phase diagram, exhibiting a variety of phases, with unusual spin, charge, lattice and orbital order. On the other hand, the high Curie temperature and especially high magnetoresistance of these materials making the multilayer study of manganites is important as it has a direct application in electronic devices and industry.

Currently, important issues in manganite namely are; How could the magnetoresistance in manganite film and polycrystals be improved? How could the room temperature and metal-insulator transition temperature in these materials be increased? What is the effect of substrate type on physical and magneto-transport properties of these materials? What is the effect of insulator manganite if sandwiched between two metallic manganites?

In order to address these questions, we have studied  $\text{La}_{2/3}\text{Ca}_{1/3}\text{MnO}_3$  (LCMO),  $\text{La}_{5/8}\text{Sr}_{3/8}\text{MnO}_3$  (LSMO),  $\text{La}_{0.7}\text{Na}_{0.3}\text{MnO}_3$  (LNMO) and  $\text{Pr}_{0.7}\text{Ca}_{0.3}\text{MnO}_3$  (PCMO) polycrystalline bulk manganites in the form of bulk and thin films that are deposited on different substrates. In addition a LCMO/PCMO/LCMO trilayer is fabricated to study the effect of multilayers on the enhancement of magnetoresistance.

## **1.4 Objective of Thesis**

This thesis is focused on fabrication and characterization of LCMO, LSMO, LNMO and PCMO polycrystalline manganites in the form of bulk, single and trilayer thin films deposited on different substrates by Pulsed Laser Deposition (PLD) technique.

The objectives of this work are presented as follow:

- 1) To prepare and characterize high quality  $\text{La}_{2/3}\text{Ca}_{1/3}\text{MnO}_3$  (LCMO),  $\text{La}_{5/8}\text{Sr}_{3/8}\text{MnO}_3$  (LSMO),  $\text{La}_{0.7}\text{Na}_{0.3}\text{MnO}_3$  (LNMO) and  $\text{Pr}_{0.7}\text{Ca}_{0.3}\text{MnO}_3$  (PCMO) polycrystalline bulk manganites via solid state reaction method.
- 2) To prepare and characterize high quality  $\text{La}_{2/3}\text{Ca}_{1/3}\text{MnO}_3$  (LCMO),  $\text{La}_{5/8}\text{Sr}_{3/8}\text{MnO}_3$  (LSMO),  $\text{La}_{0.7}\text{Na}_{0.3}\text{MnO}_3$  (LNMO) single layer thin films grown on different substrates by PLD technique.
- 3) To investigate the magnetoresistance enhancement in LCMO/PCMO/LCMO trilayers films grown on Si-wafer by PLD method.

## **1.5 Plan of Thesis**

The thesis is arranged in the following way:

In Chapter 1, general introduction of manganites, motivation and objectives of thesis are included.

In Chapter 2, a summary of previous work and literature review of manganites are given.

In Chapter 3, an overview of theory of manganites, thin film growth methods and fundamental of laser ablation are described.

In Chapter 4, an overview of sample preparation and the deposition process are described. In addition, the basic instruments used to fabricate and characterize the samples were introduced.

Chapter 5 describes the characterization and measurement details of bulk manganites, single layer and trilayer thin films. Finally the analysis and discussion of results are presented.

In Chapter 6 conclusions and suggestions are included.

## REFERENCES

- Adams, C., Lynn, J., Smolyaninova, V., Biswas, A., Greene, R., W Ratcliff, I., Cheong, S., Mukovskii, Y., & Shulyatev, D. (2004). First-order nature of the ferromagnetic phase transition in (LaCa) MnO<sub>3</sub> near optimal doping. *Physical Review B*, 70(13), 134414-134425.
- Alessandri, I., Malavasi, L., Bontempi, E., Mozzati, M., Azzoni, C., Flor, G and Depero, L. (2004). Synthesis and characterisation of La<sub>1-x</sub>Na<sub>x</sub>MnO<sub>3+δ</sub> thin films manganites. *Materials Science and Engineering: B*, 109(1), 203-206.
- Amaral, V., Araújo, J., Pogorelov, Y. G., Sousa, J., Tavares, P., Vieira, J., Algarabel, P and Ibarra, M. (2003). Tricritical points in La-based ferromagnetic manganites. *Journal of Applied Physics*, 93(10), 7646-7648.
- Anderson, P., and Hasegawa, H. (1955). Considerations on double exchange. *Physical Review*, 100(2), 675-681.
- Anjana Dogra, Sudhindra Rayaprol, Babu, P. D., G., R. K and Gupta, S. K. (2010). Influence of chemical pressure on the magnetism of Pr<sub>0.7</sub>Ca<sub>0.3-x</sub>Sr<sub>x</sub>MnO<sub>3</sub> (x = 0.0–0.3). *Journal of Alloys and Compounds*, 493, L19-L24.
- Awana, V., Tripathi, R., Balamurugan, S., Kishan, H and Takayama-Muromachi, E. (2006). Magneto Transport of high TCR (temperature coefficient of resistance) La<sub>2/3</sub>Ca<sub>1/3</sub>MnO<sub>3</sub>: Ag Polycrystalline Composites. *Arxiv preprint cond-mat*, 0609364.
- Banerjee, A., Pal, S., and Chaudhuri, B. (2001). Nature of small-polaron hopping conduction and the effect of Cr doping on the transport properties of rare-earth manganite LaPbMnCrO. *The Journal of Chemical Physics*, 115, 1550-1558.
- Bao, Y., Gao, J., and Gawne, D. T. (2010). Crack formation and its prevention in PVD films on epoxy coatings. *Surface and Coatings Technology*, 205(1), 15-21.
- Bebenin, N., Zainullina, R., Bannikova, N., Ustinov, V and Mukovskii, Y. M. (2008). Magnetic phase transition and electronic transport in single-crystalline La<sub>0.7</sub> Ca<sub>0.3</sub> MnO<sub>3</sub>. *Physical Review B*, 78(6), 064415-064422.
- Bebenin, N., Zainullina, R., Chusheva, N., Ustinov, V and Mukovskii, Y. M. (2006). Hall effect and conductivity in La<sub>1-x</sub>B<sub>x</sub>MnO<sub>3</sub>single crystals. *Journal of Magnetism and Magnetic Materials*, 300(1), e111-e113.
- Beschoten, B., Johnston-Halperin, E., Young, D., Poggio, M., Grimaldi, J., Keller, S., DenBaars, S., Mishra, U., Hu, E and Awschalom, D. (2001). Spin coherence and dephasing in GaN. *Physical Review B*, 63(12), 121202-121206.

- Billinge, S. J. L. (2006). Structure determination and phase analysis by the use of neutron diffraction. *JOM Journal of the Minerals, Metals and Materials Society*, 58(3), 47-51.
- Biškup, N., De Andres, A., Martinez, J and Perca, C. (2005). Origin of the colossal dielectric response of  $\text{Pr}_{0.6}\text{Ca}_{0.4}\text{MnO}_3$ . *Physical Review B*, 72(2), 024115.
- Bowen, M., Barthélémy, A., Bibes, M., Jacquet, E., Contour, J. P., Fert, A., Cicacci, F., Duo, L and Bertacco, R. (2005). Spin-polarized tunneling spectroscopy in tunnel junctions with half-metallic electrodes. *Physical Review Letters*, 95(13), 137203-137207.
- Chatterji, T., Ouladdiaf, B., Mandal, P., Bandyopadhyay, B and Ghosh, B. (2002). Jahn-Teller transition in  $\text{La}_{1-x}\text{Sr}_x\text{MnO}_3$  in the low-doping region. *Physical Review B*, 66(5), 054403-054411.
- Chen, Y., and Wu, T. (2008). Thickness dependent transport properties and percolative phase separation in polycrystalline manganite thin films. *Applied physics letters*, 93(22), 224104-224107.
- Cheong, S.W., and Hawang, H.Y.(2000). ferromagnetism vs.charge/orbital ordering in mixed-valent manganites. *colossal magnetoresistance Oxides*, 237-280.
- Choi, S. G., Reddy, A. S., Yu, B. G., Yang, W. S., Cheon, S. H and Park, H. H. (2010). Effect of high temperature post-annealing of  $\text{La}_{0.7}\text{Sr}_{0.3}\text{MnO}_3$  films deposited by radio frequency magnetron sputtering on  $\text{SiO}_2/\text{Si}$  substrates heated at low temperature. *Thin Solid Films*, 518(15), 4432-4436.
- Coey, J., Viret, M and Von Molnar, S. (1999). Mixed-valence manganites. *Advances in physics*, 48(2), 167-293.
- Coey, J. M. D., Viret, M., Ranno, L and Ounadjela, K. (1995). Electron localization in mixed-valence manganites. *Physical Review Letters*, 75(21), 3910-3913.
- Collado, J., García-Muñoz, J and Aranda, M. (2010). Effects of the A-site cation number on the properties of  $\text{Ln}_{5/8}\text{M}_{3/8}\text{MnO}_3$  manganites. *Journal of Solid State Chemistry*, 183(5), 1083-1089.
- Dan Liu , W. L. (2011). Growth and characterization of epitaxial  $(\text{La}_{2/3}\text{Sr}_{1/3})\text{MnO}_3$  films by pulsed laser deposition. *Ceramics International*, 37, 3531-3534.
- Daoudi, K., Tsuchiya, T and Kumagai, T. (2008). Growth and characterization of epitaxial  $\text{La}_{0.7}\text{Ca}_{0.3}\text{MnO}_3$  thin films by metal-organic deposition on  $(\text{LaAlO}_3)_{0.3}-(\text{SrAlTaO}_6)_{0.7}$  substrates. *Thin Solid Films*, 516(18), 6325-6329.
- Daughton, J., Pohm, A., Fayfield, R., and Smith, C. (1999). Applications of spin dependent transport materials. *Journal of Physics D: Applied Physics*, 32, R169.

- De Gennes, P. G. (1960). Effects of double exchange in magnetic crystals. *Physical Review*, 118(1), 141-154.
- De Teresa, J. M., Barthélémy, A., Fert, A., Contour, J. P., Montaigne, F and Seneor, P. (1999). Role of metal-oxide interface in determining the spin polarization of magnetic tunnel junctions. *Science*, 286(5439), 507-509.
- Dirks, A., and Leamy, H. (1977). Columnar microstructure in vapor-deposited thin films. *Thin Solid Films*, 47(3), 219-233.
- Dong, W., Zhu, X., Tao, R and Fang, X. (2006). Properties of (h 00)-oriented  $\text{La}_{1-x}\text{Na}_x\text{MnO}_3$  films ( $x= 0.1, 0.15$  and  $0.3$ ) prepared by chemical solution deposition method. *Journal of Crystal Growth*, 290(1), 180-184.
- Dorsey, P., Bushnell, S., Seed, R and Vittoria, C. (1993). Epitaxial yttrium iron garnet films grown by pulsed laser deposition. *Journal of Applied physics*, 74(2), 1242-1246.
- Eason, R. (2007). *Pulsed laser deposition of thin films: applications-led growth of functional materials*: Wiley-Blackwell.
- Emin, D., and Holstein, t. (1976). Adiabatic theory of an electron in a deformable continuum. *Physical review Letters*, 36(6), 323.
- Eerenstein, W., Wiora, M., Prieto, J., Scott, J and Mathur, N. (2007). Giant sharp and persistent converse magnetoelectric effects in multiferroic epitaxial heterostructures. *Nature materials*, 6(5), 348-351.
- Fang, S., Zhiyong Pang, F. W., Liang Lin and Shenghao Han (2011). Annealing Effect on Transport and Magnetic Properties of  $\text{La}_{0.67}\text{Sr}_{0.33}\text{MnO}_3$  Thin Films Grown on Glass Substrates by RF Magnetron Sputtering. *J. Mater. Sci. Technol*, 27(3), 223-226.
- Fontcuberta, J., Martinez, B., Seffar, A., Pinol, S., Garcia-Munoz, J and Obradors, X. (1996). Colossal magnetoresistance of ferromagnetic manganites: Structural tuning and mechanisms. *Physical Review Letters*, 76(7), 1122-1125.
- Gajek, M., Bibes, M., Fusil, S., Bouzehouane, K., Fontcuberta, J., Barthélémy, A and Fert, A. (2007). Tunnel junctions with multiferroic barriers. *Nature materials*, 6(4), 296-302.
- Geohegan, D., Chrisey, D and Hubler, G. (1994). Pulsed laser deposition of thin films. *eds DB Chrisey, GK Hubler, John Wiley and Sons, Inc*, 613.
- Geohegan, D. B. (1992). Fast intensified-CCD photography of  $\text{YBa}_2\text{Cu}_3\text{O}_{7-x}$  laser ablation in vacuum and ambient oxygen. *Applied physics letters*, 60(22), 2732-2734.

- Goldschmidt, V. (1926). The laws of crystal chemistry. *Naturwissenschaften*, 14, 477-485.
- Gomes, I., Almeida, B., Lopes, A., Araújo, J., Barbosa, J and Mendes, J. (2010). Structural and magnetic characterization of LaSrMnO<sub>3</sub> thin films deposited by laser ablation on MgO substrates. *Journal of Magnetism and Magnetic Materials*, 322(9), 1174-1177.
- Gregg, J., Petej, I., Jouguet, E., & Dennis, C. (2002). Spin electronics-a review. *Journal of Physics D: Applied Physics*, 35, R121.
- Gupta, A., Gong, G., Xiao, G., Duncombe, P., Lecoer, P., Trouilloud, P., Wang, Y., Dravid, V and Sun, J. (1996). Grain-boundary effects on the magnetoresistance properties of perovskite manganite films. *Physical Review B*, 54(22), 15629-15632.
- Gupta, A., and Sun, J. (1999). Spin-polarized transport and magnetoresistance in magnetic oxides. *Journal of Magnetism and Magnetic Materials*, 200(1), 24-43.
- Haghir-Gosnet, A., and Renard, J.(2003). CMR maganites: Physics, thin film and devices, *Journal of physics D: Applied physics*,36, R127-R150
- Holstein, T. (1959). Studies of polaron motion: Part II. The “small” polaron. *Annals of Physics*, 8(3), 343-389.
- Huang, Q., Santoro, A., Lynn, J., Erwin, R., Borchers, J., Peng, J., Ghosh, K., and Greene, R. (1998). Structure and magnetic order in La<sub>1-x</sub>Ca<sub>x</sub>MnO<sub>3</sub> (0< x<= 0.33). *Physical Review B*, 58, 2684-2691.
- Hwang, H., Cheong, S., Ong, N and Batlogg, B. (1996). Spin-Polarized Intergrain Tunneling in La<sub>2/3</sub>Sr<sub>1/3</sub> MnO<sub>3</sub>. *Physical Review Letters*, 77(10), 2041-2044.
- Hwang, H., Cheong, S., Radaelli, P., Marezio, M and Batlogg, B. (1995). Lattice Effects on the Magnetoresistance in Doped LaMnO<sub>3</sub>. *Physical Review Letters*, 75(5), 914-917.
- Ishii, Y., Yamada, H., Sato, H., Akoh, H., Ogawa, Y., Kawasaki, M and Tokura, Y. (2006). Improved tunneling magnetoresistance in interface engineered (La, Sr) MnO junctions. *Applied physics letters*, 89, 042509-042514.
- Jahn, H. A., and Teller, E. (1937). Stability of polyatomic molecules in degenerate electronic states. I. Orbital degeneracy. *Proceedings of the Royal Society of London. Series A, Mathematical and Physical Sciences*, 161(905), 220-235.

- Jin, S., Tiefel, T. H., McCormack, M., Fastnacht, R., Ramesh, R and Chen, L. (1994). Thousandfold change in resistivity in magnetoresistive La-Ca-Mn-O films. *Science*, 264(5157), 413-415.
- Jonker, G., and Van Santen, J. (1950). Ferromagnetic compounds of manganese with perovskite structure. *Physica*, 16(3), 337-349.
- Ju, H. G., J.;Peng, JL;Li, Q.;Xiong, GC.;Venkatesan, T.;Greene, RL (1995). Dependence of giant magnetoresistance on oxygen stoichiometry and magnetization in polycrystalline  $\text{La}_{0.67}\text{Ba}_{0.33}\text{MnO}_z$ . *Physical Review B*, 51(9), 6143-6146.
- Kalyana, L.Y., and Venugopal , R.P., (2009). Influnce of sintering temperature and oxygen stoichiometry on electrical transport properties of  $\text{La}_{0.67}\text{Na}_{0.33}\text{MnO}_3$  manganites. *Journal of Alloy and compounds*, 470(1), 67-74.
- Kramers, H. (1934). L'interaction entre les atomes magnétogènes dans un cristal paramagnétique. *Physica*, 1, 182-192.
- Lebedev, O., Van Tendeloo, G., Amelinckx, S., Leibold, B., and Habermeier, H. U. (1998). Structure and microstructure of  $\text{La}_{1-x}\text{Ca}_x\text{MnO}_{3-\delta}$  thin films prepared by pulsed laser deposition. *Physical Review B*, 58(12), 8065-8074.
- Leufke, P. M., and Ajay Kumar Mishra , A. B., Di Wang , Christian Kübel ,Robert Kruk , Horst Hahn (2012). Large-distance rf- and dc-sputtering of epitaxial  $\text{La}_{1-x}\text{Sr}_x\text{MnO}_3$  thin films. *Thin Solid Films*, 520(17), 5521-5527.
- Leung, Y., and Wong, K. (1998). Low temperature processing of epitaxial  $\text{La}_{1-x}\text{Ca}_x\text{MnO}_3$  thin films by pulsed laser deposition. *Applied Surface Science*, 127, 491-495.
- Li, H., Fang, Q and Zhu, Z. (2002a). Preparation and colossal magnetoresistance in a trilayer  $\text{La}_{0.67}\text{Sr}_{0.33}\text{MnO}_3/\text{La}_{0.75}\text{MnO}_3/\text{La}_{0.67}\text{Sr}_{0.33}\text{MnO}_3$  device by dc magnetron sputtering. *Materials Research Bulletin*, 37(5), 859-866.
- Li, H., Sun, J and Wong, H. (2002b). Enhanced low-field magnetoresistance in  $\text{La}_{2/3}\text{Ca}_{1/3}\text{MnO}_3/\text{Pr}_{2/3}\text{Ca}_{1/3}\text{MnO}_3$  superlattices. *Applied physics letters*, 80(4), 628-630.
- Li, P., Yuan, S., Liu, L., Wang, X., Wang, Y., Tian, Z., He, J., Yuan, S., Liu, K., Ying, S and Wang, C. (2008). Effect of grain boundary on electrical, magnetic and magnetoresistance properties in  $\text{La}_{2/3}\text{Ca}_{1/3}\text{MnO}_3/\text{CuMn}_2\text{O}_4$  composites. *Solid State Communications*, 146, 515-521.

- Licci, F., Turilli, G., Ferro, P and Ciccarone, A. (2003). Low-Temperature Synthesis and Properties of  $\text{LaMnO}_{3\pm d}$  and  $\text{La}_{0.67}\text{R}_{0.33}\text{MnO}_{3\pm d}$  ( $\text{R} = \text{Ca}, \text{Sr}, \text{Ba}$ ) from Citrate Precursors. *Journal of the American Ceramic Society*, 86(3), 413-419.
- Liu,D., and Liu,W. (2012). Room temperature ultrahigh magnetoresistance nanostructure  $\text{La}_{2/3}\text{Sr}_{1/3}\text{MnO}_3$  films on  $\text{SrTiO}_3$  substrate. *Ceramics International*, 38(3), 2579-2581
- Lu, W., Luo, X., Hao, C., Song, W and Sun, Y. (2008). Magnetocaloric effect and Griffiths-like phase in  $\text{La}_{0.67}\text{Sr}_{0.33}\text{MnO}_3$  nanoparticles. *Journal of Applied Physics*, 104(11), 113908.
- Ma, X., Zhang, H., Xu, J., Niu, J., Yang, Q., Sha, J and Yang, D. (2002). Synthesis of  $\text{La}_{1-x}\text{Ca}_x\text{MnO}_3$  nanowires by a sol-gel process. *Chemical physics letters*, 363(5), 579-582.
- Maity, S., Dhar, A., Ray, S., & Bhattacharya, D. (2011). Role of growth temperature and oxygen partial pressure on the structural and electrical properties of pulsed laser deposited  $\text{La}_{1-x}\text{Sr}_x\text{MnO}_{3-x}$  thin films. *Journal of Physics and Chemistry of Solids*, 72, 804-809.
- Majumdar, S., H. Huhtinen, H. S. M., P. Paturi (2012). Stress and defect induced enhanced low field magnetoresistance and dielectric constant in  $\text{La}_{0.7}\text{Sr}_{0.3}\text{MnO}_3$  thin films. *Journal of Alloys and Compounds*, 512, 332-339.
- Malavasi, L., Mozzati, M. C., Alessandri, I., Affronte, M., Cervetto, V., Azzoni, C. B and Flor, G. (2004). Thin films of sodium-doped lanthanum manganites: role of substrate and thickness on the magnetoresistive response. *Solid state ionics*, 172(1), 265-269.
- Mao, S. S., Mao, X., Greif, R and Russo, R. E. (2000). Initiation of an early-stage plasma during picosecond laser ablation of solids. *Applied physics letters*, 77, 2464-2466.
- Martin, L., Chu, Y. H and Ramesh, R. (2010). Advances in the growth and characterization of magnetic, ferroelectric, and multiferroic oxide thin films. *Materials Science and Engineering: R: Reports*, 68(4), 89-133.
- Metev, S. (1994). Process characteristics and film properties in pulsed laser deposition. *Pulsed Laser Deposition of thin films*, 229-254.
- Mira, J., Rivas, J., Hueso, L., Rivadulla, F., Quintela, M. A. L., Rodríguez, M. A. S and Ramos, C. (2001). Strong reduction of lattice effects in mixed-valence manganites related to crystal symmetry. *Physical Review B*, 65(2), 024418-024423.
- Mott, I. G. A. a. N. F. (1969). Polarons in crystalline and non-crystalline materials. *Advanced in Physics*, 18(71), 41-102.

- Ohring, M. (2002). *The materials science of thin films*: Academic Press, San Francisco.
- Okuda, T., Tomioka, Y., Asamitsu, A and Tokura, Y. (2000). Low-temperature properties of  $\text{La}_{1-x}\text{Ca}_x\text{MnO}_3$  single crystals: Comparison with  $\text{La}_{1-x}\text{Sr}_x\text{MnO}_3$ . *Physical Review B*, 61(12), 8009-8015.
- Pankova', M. S., and Chromik, S'., Sedla'c'kova', I. V. v., K. , Lobotka, P. , Lucas, S., and Stanc'ek, S. (2007). Epitaxial LSMO films grown on MgO single crystalline substrates. *Applied Surface Science*, 253, 7599-7603.
- Panwar , N., Sen , V., D.K. Pandya and Agarwal, S. K. (2007). Grain boundary effects on the electrical and magnetic properties of  $\text{Pr}_{2/3}\text{Ba}_{1/3}\text{MnO}_3$  and  $\text{La}_{2/3}\text{Ca}_{1/3}\text{MnO}_3$  manganites. *Materials Letters*, 61, 4879-4883.
- Pi, L., Zheng, L and Zhang, Y. (2000). Transport mechanism in polycrystalline  $\text{La}_{0.825}\text{Sr}_{0.175}\text{Mn}_{1-x}\text{Cu}_x\text{O}_3$ . *Physical Review B*, 61(13), 8917-8921.
- Qin, H., Hu, J., Chen, J., Zhu, L and Niu, H. (2004). The Nd Doping Effect on the Room Temperature Magnetoresistance in Manganites  $(\text{La}_{1-x}\text{Nd}_x)_{0.67}\text{Sr}_{0.33}\text{MnO}_3$  ( $x=0.3$ ). *Materials Transactions*, 45(4), 1251-1254.
- Qin, H., Hu, J., Chen, J., Zhu, L and Niu, H. (2010). Advances in the growth and characterization of magnetic, ferroelectric, and multiferroic oxide thin films. *Materials Science and Engineering: R: Reports*, 68(4), 89-133.
- Ramirez, A. (1997). Colossal magnetoresistance. *Journal of Physics: Condensed Matter*, 9, 8171-8199.
- Ramirez, A., Schiffer, P., Cheong, S., Chen, C., Bao, W., Palstra, T., Gammel, P., Bishop, D and Zegarski, B. (1996). Thermodynamic and Electron Diffraction Signatures of Charge and Spin Ordering in  $\text{La}_{1-x}\text{Ca}_x\text{MnO}_3$ . *Physical Review Letters*, 76(17), 3188-3191.
- Rijnders, G., and Blank, D. H. A. (2006). Growth Kinetics During Pulsed Laser Deposition. *Pulsed Laser Deposition of thin films*, 177-190.
- Rivadulla, F., Rivas, J and Goodenough, J. (2004). Suppression of the magnetic phase transition in manganites close to the metal-insulator crossover. *Physical Review B*, 70(17), 172410-172413.
- Roy, S., Dubenko, I., Edorh, D. D and Ali, N. (2004). Size induced variations in structural and magnetic properties of double exchange  $\text{LaSrMnO}$  nano-ferromagnet. *Journal of Applied physics*, 96, 1202.
- Ruotolo, A., Miletto Granozio, F., Oropallo, A., Pepe, G., Perna, P., Scotti di Uccio, U., Pullini, D., Innocenti, G and Perlo, P. (2007). Novel low-field magnetoresistive devices based on manganites. *Journal of Magnetism and Magnetic Materials*, 310(2), e684-e686.

- Sahana, M., Hegde, M., Shivakumara, C., Prasad, V and Subramanyam, S. (1999). Colossal magnetoresistance in potassium doped lanthanum manganite: a comparative study of polycrystalline solid and thin film. *Journal of Solid State Chemistry*, 148(2), 342-346.
- Sahu, D., Mishra, D., Huang, J. L and Roul, B. (2007). Annealing effect on the properties of  $\text{La}_{0.7}\text{Sr}_{0.3}\text{MnO}_3$  thin film grown on Si substrates by DC sputtering. *Physica B: Condensed Matter*, 396(1-2), 75-80.
- Sahu, D., Mishra, D., Hung, S., Pramanik, P and Roul, B. (2007).  $\text{La}_{0.67}\text{Ca}_{0.33}\text{MnO}_3$  thin films on Si (100) by DC magnetron sputtering technique using nanosized powder compacted target. *Materials Research Bulletin*, 42(6), 1119-1127.
- Sahu, D. R. (2012).  $\text{La}_{0.7}\text{Sr}_{0.3}\text{MnO}_3$  film prepared by dc sputtering on silicon substrate: Effect of working pressure. *Journal of Physics and Chemistry of Solids*, 73, 622-625.
- Sahua, D. R. (2010). Lateral parameter variations on the properties of  $\text{La}_{0.7}\text{Sr}_{0.3}\text{MnO}_3$  films prepared on Si (100) substrates by dc magnetron sputtering. *Journal of Alloys and Compounds*, 503, 163-169.
- Salamon, M. B., and Jaime, M. (2001). The physics of manganites: Structure and transport. *Reviews of Modern Physics*, 73(3), 583.
- Schramm, S., Hoffmann, J., and Jooss, C. (2008). Transport and ordering of polarons in CER manganites  $\text{PrCaMnO}$ . *Journal of Physics: Condensed Matter*, 20, 395231.
- Shinde, K., Pawar, S., Shirage, P and Paward, S. (2012). Studies on morphological and magnetic properties of  $\text{La}_{1-x}\text{Sr}_x\text{MnO}_3$ . *Applied Surface Science*, 258(19), 7417-7420.
- Sirenaa, M., N. Haberkorna, M. G., L.B. Steren, J. Guimpel (2004). Oxygen and disorder effect in the magnetic properties of manganite films. *Journal of Magnetism and Magnetic Materials*, 272-276, 1171-1173.
- Snyder, G. J., Hiskes, R., DiCarolis, S., Beasley, M. R and Geballe, T. H. (1996). Intrinsic electrical transport and magnetic properties of  $\text{La}_{0.67}\text{Ca}_{0.33}\text{MnO}_3$  and  $\text{La}_{0.67}\text{Sr}_{0.33}\text{MnO}_3$  MOCVD thin films and bulk material. *Physical Review B*, 53(21), 14434.
- Solanki, P., Doshi, R., Khachar, U., Choudhary, R., & Kuberkar, D. (2011). Thickness dependent transport and magnetotransport in CSD grown  $\text{La}_{0.7}\text{Pb}_{0.3}\text{MnO}_3$  manganite films. *Materials Research Bulletin*, 46(7), 1118-1123.
- Spankova, M., Chromik, S., Vavra, I., Sedlackova, K., Lobotka, P., Lucas, S and Stancek, S. (2007). Epitaxial LSMO films grown on MgO single crystalline substrates. *Applied Surface Science*, 253(18), 7599-7603.

- Steren, L., Sirena, M and Guimpel, J. (2000). Substrate influence on the magnetoresistance and magnetic order in  $\text{La}_{0.6}\text{Sr}_{0.4}\text{MnO}_3$  films. *Journal of Magnetism and Magnetic Materials*, 211(1), 28-34.
- Tang, G., Yu, Y., Chen, W and Cao, Y. (2008). The electrical resistivity and thermal infrared properties of  $\text{La}_{1-x}\text{Sr}_x\text{MnO}_3$  compounds. *Journal of Alloys and Compounds*, 461(1), 486-489.
- Tao, R., Fang, X., Dong, W., Deng, Z., Pu, T and Zhu, X. (2007). Processing effects on the chemical solution deposition-derived  $\text{La}_{2/3}\text{Ca}_{1/3}\text{MnO}_3$  films on  $\text{SrTiO}_3$  (0 0 1) substrates. *Journal of Crystal Growth*, 306(2), 356-360.
- Tao Wang , X. F., Weiwei Dong, Ruhua Tao , Zanhong Deng,Da Li , Yiping Zhao, Gang Meng, Shu Zhou, Xuebin Zhu (2008). Mechanochemical effects on microstructure and transport properties of nanocrystalline  $\text{La}_{0.8}\text{Na}_{0.2}\text{MnO}_3$  ceramics. *Journal of Alloys and Compounds*, 428, 248-252.
- Teplykh, A., Bogdanov, S., Valiev, E., Pirogov, A., Dorofeev, Y. A., Ostroushko, A., Udilov, A and Kazantzev, V. (2004). Size effect in nanocrystalline manganites  $\text{La}_{1-x}\text{A}_x\text{MnO}_3$  with A= Ag, Sr. *Physica B: Condensed Matter*, 350(1), 55-58.
- Tokura, Y. (2006). Critical features of colossal magnetoresistive manganites. *Reports on Progress in Physics*, 69, 797.
- Tomioka, Y., Koshimizu, M and Asai, K. (2009). Positron lifetime study of  $\text{Pr}_{1-x}\text{Ca}_x\text{MnO}_3$  ( $x = 0.5, 0.3$ ) during magnetic transition. *Radiation Physics and Chemistry*, 78, 1092-1095.
- Tripathi, R., Awana, V., Panwar, N., Bhalla, G., Habermier, H., Agarwal, S and Kishan, H. (2009). Enhanced room temperature coefficient of resistance and magnetoresistance of Ag-added  $\text{La}_{0.7}\text{Ca}_{0.3-x}\text{Ba}_x\text{MnO}_3$  composites. *Journal of Physics D: Applied Physics*, 42, 175002.
- Urushibara, A., Moritomo, Y., Arima, T., Asamitsu, A., Kido, G andTokura, Y. (1995). Insulator-metal transition and giant magnetoresistance in  $\text{La}_{1-x}\text{Sr}_x\text{MnO}_3$ . *Physical Review B*, 51(20), 14103-14109.
- Van Santen, J., and Jonker, G. (1950). Electrical conductivity of ferromagnetic compounds of manganese with perovskite structure. *Physica*, 16, 599-600.
- Varshney, D., Dodiya, N and Shaikh, M. W. (2011). Structural properties and electrical resistivity of Na-substituted lanthanum manganites:  $\text{La}_{1-x}\text{Na}_x\text{MnO}_{3+y}$  ( $x= 0.1, 0.125$  and  $0.15$ ). *Journal of Alloys and Compounds*, 509(27), 7447-7457.

- Venimadhav, A., Hegde, M., Prasad, V., and Subramanyam, S. (2000). Enhancement of magnetoresistance in manganite multilayers. *Journal of Physics D: Applied Physics*, 33, 2921.
- Venimadhav, A., Hegde, M., Rawat, R., Das, I and El Marssi, M. (2001). Enhancement of magnetoresistance in  $\text{La}_{0.67}\text{Ca}_{0.33}\text{MnO}_3/\text{Pr}_{0.7}\text{Ca}_{0.3}$  Mn<sub>3</sub>epitaxial multilayers. *Journal of Alloys and Compounds*, 326(1), 270-274.
- Venkataiah, G., Krishna, D., Vithal, M., Rao, S., Bhat, S., Prasad, V., Subramanyam, S and Reddy, P. V. (2005). Effect of sintering temperature on electrical transport properties of  $\text{La}_{0.67}\text{Ca}_{0.33}\text{MnO}_3$ . *Physica B: Condensed Matter*, 357(3), 370-379.
- Venkataiah, G., Prasad, V., and Venugopal Reddy, P. (2007). Influence of A-site cation mismatch on structural, magnetic and electrical properties of lanthanum manganites. *Journal of Alloys and Compounds*, 429(1), 1-9.
- Vertruyen, B., Dusoulier, L., Fagnard, J. F., Vanderbemden, P., Vanhooyland, G., Ausloos, M., Delwiche, J., Rulmont, A and Cloots, R. (2004). Anisotropic behaviour in the magnetic field dependence of the low temperature electrical resistance of calcium-doped lanthanum manganate thin films grown by RF magnetron sputtering. *Journal of Magnetism and Magnetic Materials*, 280(2), 264-272.
- Vincent, H., Audier, M., Pignard, S and DeZanneau, G. (2002). Crystal Structure Transformations of a Magnetoresistive  $\text{La}_{0.8}\text{MnO}_{3-\delta}$  Thin Film. *Journal of Solid State Chemistry*, 164(2), 177-187.
- Viret, M., Ranno, L., and Coey, J. (1997). Magnetic localization in mixed-valence manganites. *Physical Review B*, 55(13), 8067.
- Vlakhov, E., Nenkov, K., Donchev, T., Mateev, E., and Chakalov, R. (2004). Ferromagnetic and charge ordering competition in strained thin films of  $\text{La}_{1-x}\text{Ca}_x\text{MnO}_3$  system. *Vacuum*, 76(2-3), 249-252.
- Von Helmolt, R., Wecker, J., Holzapfel, B., Schultz, L., and Samwer, K. (1993). Giant negative magnetoresistance in perovskitelike  $\text{La}_{2/3}\text{Ba}_{1/3}\text{MnO}_x$  ferromagnetic films. *Physical Review Letters*, 71(14), 2331-2333.
- Williamson, G., and Hall, W. (1953). X-ray line broadening from filed aluminium and wolfram. *Acta Metallurgica*, 1(1), 22-31.
- Wolf, S., Awschalom, D., Buhrman, R., Daughton, J., Von Molnar, S., Roukes, M., Chtchelkanova, A and Treger, D. (2001). Spintronics: A spin-based electronics vision for the future. *Science*, 294(5546), 1488-1495.

- Wu, B. (2008). High-intensity nanosecond-pulsed laser-induced plasma in air, water, and vacuum: A comparative study of the early-stage evolution using a physics-based predictive model. *Applied physics letters*, 93, 101104.
- Wu, C., Qiu, J., Wang, J., Xu, M and Wang, L. (2010). Thermochromic property of  $\text{La}_{0.8}\text{Sr}_{0.2}\text{MnO}_3$  thin-film material sputtered on quartz glass. *Journal of Alloys and Compounds*, 506(2), L22-L24.
- Xiong, C., Xiong, Y., Meng, G., Jian, Z., Mai, Y., Xu, W., Xiong, J., Zhang, L., Ren, Z and Zhang, J. (2007). Structural study and magnetoresistance effect of epitaxial  $\text{La}_{0.67}\text{Sr}_{0.33}\text{MnO}_3$ - $\delta$  and  $\text{Pr}_{0.7}\text{Ca}_{0.3}\text{MnO}_{3-\delta}$  multilayer films. *Physica B: Condensed Matter*, 390(1), 28-33.
- Xiong, Y., Xu, W., Mai, Y., Pi, H., Sun, C., Bao, X., Huang, W., & Xiong, C. (2008). The microstructure and electronic transport properties of mechanical milled  $\text{La}_{2/3}\text{Ca}_{1/3}\text{MnO}_3$  perovskites. *Journal of Magnetism and Magnetic Materials*, 320(3-4), 257-262.
- Yang, S., Kuang, W., Liou, Y., Tse, W., Lee, S and Yao, Y. (2004a). Growth and characterization of  $\text{La}_{0.7}\text{Sr}_{0.3}\text{MnO}_3$  films on various substrates. *Journal of Magnetism and Magnetic Materials*, 268(3), 326-331.
- Zainullina, R., Bebenin, N., Ustinov, V., Mukovskii, Y. M and Shulyatev, D. (2007). Phase transitions in  $\text{La}_{1-x}\text{Ca}_x\text{MnO}_3$  single crystals. *Physical Review B*, 76(1), 014408-014411.
- Zener, C. (1951). Interaction between the d-sells in the transition metals.II.Ferromagnetic compounds of manganese with perovskite structure. *Physical Review*, 82(3), 403-405
- Zhang, Q., Nakagawa, T and Saito, F. (2000). Mechanochemical synthesis of  $\text{La}_{0.7}\text{Sr}_{0.3}\text{MnO}_3$  by grinding constituent oxides. *Journal of Alloys and Compounds*, 308(1), 121-125.
- Zhao, K., Feng, J., Huang, Y., Li, H and Wong, H. K. (2005). Magnetic coupling in  $\text{La}_{0.67}\text{Ca}_{0.33}\text{MnO}_3/\text{La}_{0.67}\text{Sr}_{0.33}\text{CoO}_3/\text{La}_{0.67}\text{Ca}_{0.33}\text{MnO}_3$  sandwiches. *Thin Solid Films*, 476(2), 326-330.
- Zheng, X., Wang, C and Zhu, J. (2003). Effect of columnar structure on magnetoresistivity properties of  $\text{La}_{0.8}\text{MnO}_3$  thin films. *Journal of Magnetism and Magnetic Materials*, 267(2), 168-172.
- Zhou, Y., Wu, B and Forsman, A. (2010). Time-resolved observation of the plasma induced by laser metal ablation in air at atmospheric pressure. *Journal of Applied Physics*, 108(9), 093504-093507.
- Zhu, X and Honglie Shen, K. T., Takeshi Yanagisawa, Mamoru Okutomi, Noboru Higuchi (2012). Characterization of  $\text{La}_{0.67}\text{Sr}_{0.33}\text{MnO}_z$  thin films synthesized by

- metal-organic decomposition on different substrates. *Ceramics International* 94(9), 2783-2787.
- Žutić, I., Fabian, J and Sarma, S. D. (2004). Spintronics: Fundamentals and applications. *Reviews of Modern Physics*, 76(2), 323.



## **BIODATA OF STUDENT**

Manizheh Navasery was born on the 22<sup>th</sup> December 1971 in Ahvaz, IRAN. She received her primary school in Ahvaz from 1977 to 1982, her secondary school was continued in Hadaf high School from 1982 – 1990. She continued her university education in B. Sc. Degree in Applied Physics at Shahid Chamran University in Ahvaz and graduate in 1997. In 1997 she continued as a Master student in field of Superconductivity at Shahid Chamran University and graduate in 2000. She married on August 2006. Finally she entered University Putra Malaysia in July 2008 for PhD studying in field of Magnetic Materials.

## LIST OF PUBLICATION

### • JOURNAL PUBLICATION

- **M. Navasery, S.A. Halim, S.K.Chen, K.P.Lim, R.A.Shukor,** Structure, Electrical Transport and Magneto-Resistance properties of  $\text{La}_{5/8}\text{Ca}_{3/8}\text{MnO}_3$  Synthesized with different manganese precursors, *Modern Physics Letter B*, Vol.26, No.6, **2012**.
- **M. Navasery, S.A. Halim, S.K.Chen, K.P.Lim** “High Curie temperature for  $\text{La}_{5/8}\text{Sr}_{3/8}\text{MnO}_3$  thin films prepared by Pulsed Laser Deposition grown on glass substrate” *Journal of Physics: International Journal of Electrochemical Science*, 8, **2013**(Accepted).
- **M. Navasery, S.A. Halim, S.K.Chen, K.P.Lim** “Characterization and mechanism of  $\text{La}_{5/8}\text{Sr}_{3/8}\text{MnO}_3$  thin filmsPrepared by Pulsed Laser Deposition on different Substrates” *International Journal of Electrochemical Science*, 8, **2013** (Accepted).

### • CONFERENCE PRESENTATION

### • INTERNATIONAL CONFERENCE

- **M. Navasery, S.A. Halim, S.K.Chen, K.P.Lim, R.A.Shukor,** Growth and characterization of  $\text{La}_{5/8}\text{Ca}_{3/8}\text{MnO}_3$  film prepared by pulsed laser deposition on silicon wafer substrate, presented in “The seven international of magnetic and

superconducting materials (MSM11) at Avillion Resort Hotel, Port Dickson ,Negeri Sembilan on 10<sup>th</sup>-13<sup>th</sup> October 2011.

- **LOCAL CONFERENCE**

- **M. Navasery**, S.A. Halim, K.P.Lim, S.K.Chen , Study of Structure and Electrical properties of  $\text{La}_{1-x}\text{Ca}_x\text{MnO}$  (  $x=1/8, 1/3 \text{ & } 5/8$  ) polycrystalline manganites, presented in “ Fundemental Science Congress 2010, UPM on 18<sup>th</sup>-19<sup>th</sup> May 2010.
- **M. Navasery**, S.A. Halim, K.P.Lim, S.K.Chen , R.A.Shukor and N.Soltani, “ Study of Structure and Electrical Transport properties of RE  $\text{Ba}_2\text{Cu}_3\text{O}_{7-x}$  ( RE is Y, Gd and Nd) superconductors” presented in “ Fundemental Science Congress 2011, UPM on 5<sup>th</sup>- 6<sup>th</sup> July 2011.
- **M. Navasery**, S.A. Halim, K.P.Lim, S.K.Chen and R.A.Shukor, “Growth and characterization of  $\text{La}_{2/3}\text{Ca}_{1/3}\text{MnO}_3$  thin films by Pulsed laser deposition on Corning glass substrate” presented in 26<sup>th</sup> Regional Conference on Solid State Science and Technology 2011 (RCSSST 2011) at The Royal Bintang , Seremban,Negeri Sembilan on 22<sup>nd</sup>-24<sup>th</sup> Novomber2011.
- **M. Navasery**, S.A. Halim, K.P.Lim, S.K.Chen and R.A.Shukor, “Growth and characterization of  $\text{La}_{5/8}\text{Ca}_{3/8}\text{MnO}_3$  thin films by Pulsed laser deposition on Fused silica substrate” presented in “ Fundemental Science Congress 2012, UPM on 17<sup>th</sup>-18<sup>th</sup> July 2012.

- EXHIBITION AND AWARD

- Pameran Rekacipta Penyelidikan and Inovasi (PRPI 12) UPM 2012.

Abdul Halim Shaari, **Manizheh Navasery**, Chen Soo Kien and Lim Kean Pah “Enhancement of Magnetoresistance in LCMO/PCMO/LCMO Trilayers Grown on Si-Wafer by Pulsed Laser Deposition” **Silver Medal**.

- Pameran Rekacipta Penyelidikan and Inovasi (PRPI 12) UPM 2012.

Abdul Halim Shaari, Pan Kai Yap, **Manizheh Navasery**, Chen Soo Kien, Mohd Mustapha Awang Kechik, Lim Kean Pah and Wan Mohd Daud Wan Yusoff, “Room Temperature Ferromagnetic-Insulator Transition in LKMO prepared via Sol-Gel” **Silver Medal**.